Contract Number NORTHE8361-001
Issued by DEEP - Land & Water Resources Division (LWRD), 79 Elm Street, Hartford, CT 06106-5127

Project Title
Multibeam Mapping in Long Island Sound -- LISS Enhancement

Final Report
Project Period 07/29/2021 to 9/30/2024

Contractor
The Research Foundation for The State of New York
PO Box 9
Stony Brook University
Stony Brook, NY 11794-3362

Author
Roger D Flood
School of Marine and Atmospheric Sciences (SoMAS)
Stony Brook University
Stony Brook, NY 11794-5000
email: roger.flood@stonybrook.edu

January 31, 2025
Revised June 6, 2025

Multibeam Mapping in Long Island Sound -- LISS Enhancement

Introduction and Background

Benthic mapping in Long Island Sound (LIS) has long been identified as a priority need and is essential to improving science-based environmental management and mitigation decisions. Seafloor landscape maps depicting habitat structure and the ecological characteristics associated with those habitats are critical pieces of information which typically integrate information from a variety of sources including acoustic bathymetry and backscatter, sedimentary, geochemical, physical, and biological data.

Plans for systematic benthic mapping in Long Island Sound were initiated following the creation of the LIS Cable Fund (a settlement fund that resulted from issues surrounding cable infrastructure in LIS) in 2004. High-resolution multibeam bathymetry and backscatter measurement has been recognized as an important tool in the understanding of sedimentary processes and benthic habitats in a range of aquatic settings (e.g. Hughes Clarke et al., 1996; Mayer, 2006) and has been an important tool in characterizing the seabed for a range of uses in Long Island Sound (Knebel and Poppe, 2000). An important step in benthic mapping has been the collection and analysis of high-resolution (multibeam) bathymetric and acoustic backscatter data that shows seabed features and sediment distribution patterns. Multibeam bathymetric and backscatter data has been collected over a large portion of Long Island Sound as a result of over two decades of charting activities conducted by the National Ocean Survey, a branch of NOAA. NOAA completed much of their multibeam data acquisition in Long Island Sound in 2020, focusing in the far western portion of LIS. This represents a remarkable achievement by NOAA, which has resulted in accurate and up-to-date charts of Long Island Sound which are helping to make vessel operations safer in Long Island Sound. The equipment used to collect multibeam bathymetric and backscatter data has continued to improve over time, and we are learning that the data collected during NOAA surveys done before about 2004 does not have the spatial resolution in depth or acoustic backscatter that is needed for benthic habitat mapping, and also that complete (100% coverage) multibeam surveys were not always done in shallower areas. The NOAA mapping data has been supplemented by multibeam mapping surveys done by SoMAS, Stony Brook University, in the two priority areas studied by the LIS Cable Fund Seafloor Habitat Mapping Initiative in central ("LIS Pilot Study" or "Phase I") and eastern ("Phase II") Long Island Sound. A third high-priority area will be the focus of LIS Cable Fund Seafloor Habitat Mapping Initiative study "Phase III" in western Long Island Sound starting about 2021 (Figure 1). Studies in the high priority areas include the collection and analysis of extensive sedimentary, geochemical, physical, and biological data.

As of 2020, there were two large areas in central Long Island Sound, about 40 and 100 square miles (Figure 2), which lacked the high-resolution bathymetry and backscatter data necessary to support even the initial stages of benthic habitat mapping. Such high-resolution

morphological data is needed to extrapolate the results of the three high-priority areas throughout Long Island Sound, a high priority of the LIS Cable Fund. NOAA apparently does not intend to re-survey these two areas since the existing data satisfies charting requirements. The object of our present study has been to collect, process, and report on new high-resolution multibeam data in the larger (~100 square miles; south of New London) of these two areas to enhance the benthic habitat studies being undertaken as part of the LIS Cable Fund Seafloor Habitat Mapping Initiative. After the study LISS Enhancement study was supported, the LIS Cable Fund designated this area as "Phase IV" and designated our mapping task as "Phase IV A," the first scheduled task in the Phase IV study. Our project will help us to gain new insights into the sedimentary processes that are occurring over large areas of central Long Island Sound as well as also enable future similar studies or new research initiatives in Long Island Sound and surrounding areas.

Methods

Data Acquisition

A Kongsberg Multibeam EM2040P MKII (portable processing unit version), a Kongsberg Seapath 130-5+ GNSS (GPS) /navigation unit and a motion sensor (MRU) in a submersible housing were acquired for this project. The system includes a Fugro receiver that obtains GNSS (GPS) corrections from a geosynchronous satellite which results in higher-resolution horizontal and vertical position fixes. Other system components include an AML-3 LGR SVP 500m sound velocity profiler with depth, SV and CTD sensors to make vertical profiles of sound velocity and water properties. The velocity profile is recorded internally, an integrated GPS records the position of the cast, and the cast is downloaded over WI-FI after the profiler is recovered. We also use a Trimble BX982 GNSS receiver which can utilize RTN corrections transmitted by land stations, if cellular network signals are available, for high-resolution fixes as a backup for the Seapath position data. The states of New York and Connecticut both operate networks of land-based CORS/RTN stations (NYSNet is operated by NYSDOT and ACORN is operated by UCONN) which provide the needed GPS corrections over cellular networks. Kongsberg SIS5 and Seapath software manage the multibeam, navigation system, and motion sensors, and a Dell Rugged 5424 laptop computer runs the software and records the survey data. Survey data is copied to disk drives or RAID arrays at frequent intervals during the survey for backup and for offline processing. A monitor is installed on the bridge of the ship that displays the vessels position with respect to the desired vessel track to assist the helmsman in following the desired track. That display is attached to a second Dell 5424 laptop, which runs the Helmsman software program. The SIS5 software now can interface with the autopilot of the survey vessel and can send commands to the autopilot to steer the vessel along the track. This feature was not used during all project surveys because the helmsman display on

the bridge provides the real-time position information the helmsman needs to follow the proposed survey track. The equipment is connected to an uninterruptible power supply (UPS) so that the equipment continues to operate when the vessel power is interrupted such as when the vessel power switches from an onboard generator to shore power.

The multibeam sonar is also known as a swath mapper since it collects a swath of water depths that is perpendicular to the ship track (Figure 3). The outgoing sound pulse is narrow in the fore-aft direction but wide in the cross-track direction. The echo that is returned from the seafloor is recorded by an array of transducers which listen in narrow bands in the cross-track direction and can determine the travel time and amplitude of the echo from the seafloor where the transmit and any of the receive beam patterns overlap. The multibeam sonar used in this study can record up to 512 travel times, or depths, for each swath, although we collected 400 depths/swath during surveys in August and September and 256 depths/swath in November-December to evaluate the effects of this choice. Since the cross-track angles of the receive beams are known, the depths and cross-track distance for each beam can be calculated. Also, our system has "dual swath" capability which means that the system can transmit two sound pulses at slightly different directions in the along-track direction so that two swaths of depths can be collected each time a ping is transmitted. Collecting two swaths of depths with each ping allows the ship to collect sufficient ping density at higher ship speeds, especially in deeper water. Backscatter is the amplitude of the sound that is scattered back towards the source and the backscatter is generally thought to be related to seafloor properties such as grain size, density, roughness or sediment layering (Weber and Lorton, 2015). Backscatter data is recorded for each beam (beam backscatter) and at a higher resolution across the seafloor (time series backscatter). In addition, the system records the sonar returns in the water column itself which generates a pie-shaped image. This display is useful for observing how targets in the water column, especially individual fish and schools of fish, can affect the bottom return.

Converting travel time to water depth requires knowing the sound velocity structure in the water column and the angle of the beam from the vertical. Sound velocity (in meters per second) is needed to convert travel time (in seconds) to distance (in meters) and the angle is needed to convert the diagonal distance to vertical (water depth) and horizontal (cross-track) distance with respect to the sonar position. Sound velocity can vary with depth in the ocean since water temperature and salinity can vary with depth. Vertical changes in sound velocity can cause refractions (changes in direction of the sound pathway) and refractions caused by incorrect velocity profiles can result in incorrect depths. There can be both spatial and temporal variations in the sound velocity profile, so frequent profiles are needed to determine the correct water depth and horizontal distance for each sonar return. In this study we stopped the ship to collect a sound-velocity profile every two to four hours (for a total of 212 sound-velocity profiles), although the sound-velocity structure can change more often than that. This kind of variability is common in coastal waters where fresher waters from rivers often overlie saltier, ocean waters

and where tides and currents mix and transport water. For an estuarine setting such as Long Island Sound, fresher waters overly saltier waters to create a complex and variable velocity profile (Figure 4), and the depth, structural, spatial, and temporal variations in the sound-velocity profile can have a significant effect on the depth measurement. For our study refraction-related depth errors can be a meter or more at the outer edges of the swath. Unfortunately, there is no way to detect these kinds of changes in sound velocity without collecting many sound velocity profiles, and a measured sound velocity profile can be obsolete just minutes after it was collected. However, during post-processing, corrections can be made to reduce refraction-related depth artifacts since there is some knowledge of seafloor geometry because of adjacent and crossing sonar tracks.

The orientation, motion, and location of the vessel need to be known to determine the instantaneous angles of the different sonar beams and thus the locations of the depth and backscatter measurements on the seafloor. Our integrated navigation and motion sensor system measures vessel roll, pitch, heading, and heave (movements due mostly to waves) 100 times a second so that these corrections can be made. After the data acquisition phase of the project the multibeam manufacturer confirmed that there was a 7 to 8 millisecond delay in the timing of our motion data. This time offset was applied during post-cruise data processing. The horizontal position and the orientation of the sonar and the spatial offsets between the multibeam transducer, motion sensor, and GNSS antennas are needed to determine the locations on the seafloor where the water depths are measured. These offsets are best measured when a ship is in drydock. That wasn't possible for this project, so we made our measurements at the dock when the systems were installed. These offsets were sometimes revised during the cruise, and corrected offsets were applied during post-cruise data processing. In addition to knowing the offsets, the orientation of the multibeam transducer also needs to be precisely determined. Initial values for these orientations are refined by running a "patch test" once the system is installed and operating. Doing a roll calibration consists of running the same track in two different directions, and any difference in cross-track bottom slope on the two tracks is removed by adding a roll offset to the setup parameters. Similarly, running two or three tracks over known features on the bottom such as pipelines or sharp topography allows offsets for pitch and yaw (heading) to be determined. Occasionally the angular offsets are refined based on the features observed during the survey and updated corrections are used during post-processing of the survey data.

Precise horizontal navigation comes from the Seapath and Trimble GNSS receivers using satellite-based or land-based corrections, and positions are recorded once per second. Accurate horizontal positioning is essential, and these receivers have horizontal accuracies better than 0.1m. The fixes calculated using the Seapath GNSS are with respect to the ITRF 2014 (similar to WGS84) reference frame, while fixes calculated using the Trimble GNSS are with respect to the NAD83 reference frame. Vertical position accuracy is also important because the multibeam sonar measures water depth with respect to the transducer, so the actual elevation of the

transducer needs to be known to calculate the elevation of the seafloor. The vertical position of the transducer changes because of wave motion, and the multibeam heave sensor measures those kinds of vertical changes so depths are corrected for wave motion. Longer-term vertical movements of the ship occur because of tides and weather, especially wind speed and direction and air pressure, and those kinds of water-level changes can be measured with shore-based tide gauges and high-quality vertical GNSS data.

Vessel loading, such as taking on or using fuel, can also change to how high a ship sits in the water. The R/V *Seawolf,* one of the vessels we used during this study, has a deep draft and we could detect no elevation change when the vessel took on fuel at the midpoint of each of our two cruises. The R/V *Connecticut,* which we also used, has a shallower draft and did not refuel during our cruise. Our GNSS measurements show that the vessel rose about 0.15 m during our 13-day cruise as fuel was used. There can also be changes in vessel elevation when the vessel moves through the water. Our GNSS measurements showed that the vessel when moving was 0.1 m higher than when at rest. We kept the ship speed at between five and seven knots, which minimized vertical elevation changes due to ship speed during the survey.

Regional water-level elevations in Long Island Sound were made at coastal tidal stations operated by NOAA, USGS, and by one or more gauges deployed as part of the project. Water-level observations were also made by the GNSS receivers on the survey vessel when high-quality corrections were available. The different sources of water-level elevations were compared for this project , and we used the water-level measurements made by NOAA in New Haven, CT, (Station 8465705, https://tidesandcurrents.noaa.gov/map/index.html?id=8465705, reported as MLLW but converted to NAVD88 using VDatum) to correct soundings for water level during this study. While all the water-level observations were in agreement, the NOAA water-level measurements were less noisy, which resulted in a hillshade image that was better for interpretation. A time-varying elevation change to account for fuel use for the R/V *Connecticut* was added to the shore-based water-level change used for that survey.

Multibeam Data Processing

The SIS5 software displays the vessel tracks and does real-time gridding of the multibeam data, which helps to ensure complete coverage of the sea floor and to plan the ship tracks. However, the multibeam data needs to be processed later to ensure that the collected data is of high quality and the coverage is sufficient and to integrate observations such as coastal water levels that may not be available until later. Soon after data acquisition, we used a separate computer system on the vessel to import and post-process the multibeam data using CARIS HIPS and SIPS software, QPS Qimera software, and/or the SwathEd programs created by the Ocean Mapping Group at the University of New Brunswick. The resulting bathymetry grids can

be exported in GeoTIFF format and imported into GIS software where they can be displayed and evaluated to help with survey planning.

The survey data was reprocessed in the shore-based lab after the cruise is completed to create the final survey products. The processing steps for CARIS HIPS and SIPS (Figure 5) are similar to the processing steps used for other similar software packages. The first step is to re-evaluate the offsets between the various sensors and determine new values if necessary. The raw data files created by SIS5 are corrected for the sensor corrections used during data collection, but most offsets can be revised during post-processing. Other data sets needed at this stage are the set of sound velocity profiles and the water-level record that will be used. Each shipboard device used during the survey sends a separate message to the logging computer, and these messages are saved to a raw data file as they are received. One task of the processing software is to read the raw data files and put messages from the different sensors into different files based on instrument type. Processing the data consists of editing the data sets, for example removing spurious vessel positions or water depths, and merging the data sets together to create files with corrected depths and positions. The processed depths are used to create grids of surface elevation, which are eventually exported in GeoTIFF or another format as desired. Then there is an iterative process where tracks are selected for or removed from the project, depth and other data are edited as necessary (especially for spurious depths), anomalies are identified, water-level elevations are re-evaluated, refraction corrections are made, offsets are evaluated, and other corrections are made until, after re-merging, there are acceptable results.

The survey data for the project was collected as four distinct surveys. The four surveys were processed independently, and preliminary results of the study were provided as the results of the four surveys. Results from the four study areas were merged in ArcGIS Pro to create one file for the entire area for water depth, northwest and northeast hillshade, and backscatter.

Water Depth

Two techniques are commonly used to create the grids of surface elevation from the many point depths collected during a multibeam survey. One technique uses a Swath Angle (SA) approach, which assigns a weight to each depth based on how far the depth sounding is away from the ship track with higher weightings given to depths closer to the center of the track. The depths that fall within or near a particular grid cell are used to calculate the depth of that grid cell, and the statistics of the depths in that grid cell can be determined. The second technique used, CUBE, uses a statistical approach to determine if any sounding that falls in a particular grid cell disagrees too much with other values in the grid cell and thus should not be used. This is an effective way to filter and somewhat smooth the depth data while creating a higher-quality depth grid although the gridding step is somewhat slower than using the SA approach.

Grids for multibeam bathymetry and backscatter were created using CUBE in HIPS and SIPS version 11.4 in UTM Zone 18N with a resolution of 1 m. Those depth grids were exported as ESRI FLT format, which can be imported into ArcGIS Pro and then saved in GeoTIFF format. Since we used Seapath GNSS navigation with Fugro-supplied corrections, our positions are in the ITRF 2014 reference frame. Nautical charts published in the US and prior hydrographic surveys done after the mid-1980s use the NAD83(2011) reference frame, and our contract calls for reporting our results in the NAD83(2011) reference frame. It is possible to transform a grid in ITRF 2014 to a grid in NAD83(2011) using ArcGIS Pro, but grid transformations apparently regrid the gridded data, which can blur the image, so we sought a simpler approach to preserve detail in the gridded data. For this study we determined a local offset between the two reference frames and used that offset to shift our ITRF 2014 grid to NAD83(2011). The local offset of the two reference frames was obtained by comparing the ITRF 2014 positions of a set of NAD83(2011) locations that spanned the Phase IV study area and calculating the offsets between their UTM coordinates in the two reference frames. The UTM coordinates of the set of locations were determined using the NOAA program VDatum (https://vdatum.noaa.gov/), and we calculated that the local horizontal offset between the ITRF 2014 and NAD83(2011) UTM Zone 18N grids in the Phase IV area was 1.035 m (standard deviation 0.0012 m) in the direction 162.39º (standard deviation 0.085º). This corresponds to subtracting 0.987 m (standard deviation 0.0014 m) from the UTM Northing of the ITRF 2014 grid and adding 0.313 m (standard deviation 0.013 m) to the UTM Easting of ITRF 2014 grid. This grid shift was done in ArcGIS Pro. Any error induced by using this local offset approach is much smaller than the 1 m grid size being used. This local offset between grids seems to be applicable to all of Long Island Sound but the offset needs to be re-evaluated for any particular project or area.

Hillshade

While the depth grid and the backscatter grid provide important information about the study area, additional information about the nature of the seafloor comes from hillshade images, which are created by shining a synthetic sun across the digital depth grid and calculating the shadows that are cast by the topography. Hillshade images can show many details of the seabed morphology at a scale much smaller than can be resolved on the bathymetric grids. For this study the hillshade images were made using HIPS and SIPS and the rasters were exported as 8-bit grayscale images. Two hillshade images were made, one with the synthetic sun positioned in the northwest (sun illumination direction 315º) and one with the synthetic sun positioned in the northeast (sun illumination direction 045º). Examples of hillshade images are shown in Appendix A. A hillshade image can also be calculated in ArcGIS Pro using the Hillshade geoprocessing tool, and a bathymetry grid can also be directly displayed in ArcGIS Pro as a hillshade image in using the Shaded Relief option in Symbology. The hillshade images shown in many of the figures in this report, other than in Appendix A, were created using the Shaded Relief Symbology option.

Backscatter

There continues to be an increased focus on multibeam backscatter data acquisition, processing, and interpretation in support of habitat studies (e.g., Lurton and Lamarche, 2015). A separate set of steps is used to process the backscatter signals, and different multibeam data processing software programs follow somewhat different approaches. Our Kongsberg multibeam system can be referred to as a "calibrated" system because the properties of the electronics and sonar system are said to be known so that the amplitude of the sonar return can be determined after applying the instrumental and gain settings. The strength of the outgoing sonar pulse and the gains used in the receiving circuits are continually adjusted by the multibeam system so that the amplitude of the returned signal falls in the proper range. If gains are too high, then the returned signal values can be clipped in the electronics while if the gains are too low the software may not consistently detect the bottom return. If it is not possible to correct the recorded backscatter data for the strength of the outgoing pulse or for the gains applied to the received signal, then it may not be possible to interpret backscatter data in terms of seabed character or to compare backscatter data from different parts of a survey area.

In addition to these instrumental gain corrections, there are some other instrumental and environmental corrections that need to be made to determine how seabed reflectivity changes throughout the study area. A beam pattern correction is necessary because the transducer arrays can have different signal levels or different gains at different angles, which will result in an along-track striping in the backscatter record. The beam pattern correction is expected to be constant for a particular sonar throughout the study area. Also, the amplitude of the sound pulse changes with the distance that the pulse travels to and from the seabed because of spreading of the sound pulse in the water column and because of sound attenuation in the water column. As a result, the gain of the returned signal needs to be increased with time to account for these effects. The attenuation (expressed as dB/km) is different for different frequencies, and it changes as a function of the water temperature and salinity. For our PHASE IV stations, the average salinity was about 29 PSU, temperatures ranged from about 10º C to 24º C, and the attenuation coefficient at 300 kHz ranged from about 65 dB/km to 100 dB/km. Our maximum one-way slant range was about 100 m, so an attenuation coefficient of 65 to 100 dB/km would reduce the sonar signal strength by 13 to 20 dB. Our processing software allows us to specify one temperature and salinity per processed backscatter grid.

The angle at which sound reflects from the seafloor changes from vertical (directly beneath the ship) to a shallow angle of perhaps 70º from the vertical at the far edge of the sonar swath, and the seabed area insonified by the ping also increases from the center to edge of the swath. The seafloor is often thought of as a Lambertian surface (i.e., the backscatter decreases as the cosine-squared of the incident angle), and this kind of correction can also be considered as

part of the beam pattern correction. The intensity of the sound scattered back towards the transducer (the echo) thus decreases as the angle becomes shallower, and this can be described as the echo that approximately follows Lambert's Law. The angle between the sound pulse and the seafloor depends both on the angle of the sound pulse and the topography of the seafloor. A seabed that slopes towards the sound source at a steeper angle will have a stronger return than a seabed that slopes towards the sound source at a shallower angle or that is flat. While a Lambertian correction can be used to correct for the changing angle away from the center of the sonar swath, a different approach is needed directly beneath the ship where the sound is reflected perpendicular to the sediment surface. This change in reflectivity at the center of the swath can lead to an along-track artifact directly beneath the ship track but this effect is minimized in the data sets described here. After corrections have been made for all these effects, the backscatter map or mosaic indicates the acoustic character of the seabed material. Additional information about the acoustic properties of the seafloor materials can be investigated by measuring the angular variation of the backscatter signal (Hughes Clarke, 1994; Ferrini and Flood, 2006; Fonseca and Mayer, 2007; Lurton et al., 2018). We so far have not studied the angular variation of backscatter in the Phase IV study area.

The multibeam sonar backscatter intensity is logged as decibels (abbreviated dB), which is a logarithmic scale commonly used for acoustic measurements. The dB scale is based on the log of the ratio of the backscatter return to some reference value, often the sound intensity at 1 m from the transducer, and the logarithmic nature of the dB scale means that a dB value of 10 means that the sound intensity recorded is 10 times the reference value. Similarly, a dB value of -10 means that the sound intensity is 1/10 the reference value, a dB value of -20 means that the sound intensity is 1/100 the reference value, a dB value of -30 means that the sound intensity is 1/1000 of the reference value and so on. Also, a doubling of sound intensity corresponds to an increase of about 3 dB, and a halving of the sound intensity corresponds to a decrease of about 3 dB. In this study, the backscatter grids are represented in 32-bit floating point grids, which is the same format used for depth data. In many studies, backscatter data has been reported as 8-bit grayscale images with data values ranging from 0 to 255. Low values are often shown as black or dark gray while high values are often shown as white or light gray. The advantage of reporting the backscatter data as dB floating point grids is that the backscatter data in different grids can be combined, which is more difficult if each backscatter pixel is reported as an 8-bit grayscale value. The floating-point grids produced during this study can best be displayed in ArcGIS Pro as grayscale images with a minimum value of -20 dB and a maximum value of 5 dB, but using different minimum and maximum ranges in different areas will show more detail in backscatter variation.

We experimented with several different approaches to create our backscatter mosaics, and we decided to use the software program HIPS and SIPS from CARIS. Specifically, we used their weighted moving average (WMA) and angular-varying gain (AVG) processing option, and we

used the Beam Average backscatter data rather than the Timeseries backscatter data. Backscatter data processed using these techniques resulted in few along-track or across-track anomalies, including a much-reduced acoustic anomaly beneath the ship track. While our initial tests were successful, we had several problems using this approach on our large data sets, and much of our project effort has been directed at processing the backscatter data. In particular, the technical support desk at CARIS advised us to completely restart our multibeam processing several times when new software versions were released, and processing backscatter data for a single map could take a week or more. Eventually we were able to process the backscatter data for our large map areas in pieces and then combine the pieces in ArcGIS Pro. We could proceed with final bathymetry processing and data interpretation once we could accept our backscatter results.

Our Phase IV backscatter map at 300 kHz is relatively free of artifacts so that variations in seabed backscatter likely are due to variations in the nature of the seabed (see Weber and Lurton (2015) for a discussion of the factors that affect multibeam backscatter). The acoustic reflectivity of the seafloor depends in part on the acoustic impedance of the seafloor materials and how that differs from the acoustic impedance of the overlying water. Acoustic impedance is the product of sound velocity multiplied by density, so the acoustic impedance of seawater is about 1,500 m/s multiplied by 1,000 kg/m^3 which is 1.5x10^6 Pa-s/m. Recently or rapidly deposited, uncompacted fine-grained sediments can have sound speeds and densities that are similar to those of seawater, and thus we expect low backscatter for those sediments. Normally compacted fine-grained sediments are expected to have sound velocities and densities higher than that of seawater, and sound velocity and density also tends to be higher when there is more coarser material in the fine-grained sediments. Sandy sediments can have quite high acoustic impedances. Surface roughness also plays an important role in acoustic backscatter. The wavelength of sound at 300 kHz is about 0.5 mm which is the size of medium to coarse sand. The seabed can act as a smooth interface if the roughness elements are smaller than the sound wavelength or as a rough interface if the roughness elements are larger than the sound wavelength, so backscatter should be higher for a rougher, coarse-grained sediment than for a smoother, finer-grained sediment. The coarser materials include coarse sand, gravel, and shell fragments, which tend to have higher backscatter. Coarser materials can often be found buried in fine-grained sediments, and the sound frequencies used for the multibeam echosounder can penetrate a small distance into fine-grained sediments. Backscatter can thus be affected by the presence of coarser materials, including shell, gas bubbles, or even coarser sediment layers buried in fine-grained sediments, and the term volume scattering is used to refer to the presence of scatters within the sediment. Not all roughness elements are due to the nature of the sedimentary materials, and surface features such as sand ripples or biologically created mounds can also affect backscatter. For two-dimensional features such as sand ripples there may also be different amounts of backscatter when the sound comes from different directions.

This discussion of backscatter highlights the physical factors that contribute to the backscatter measurement. Our interest here is in benthic habitat, so it is important to note that many of the factors that affect sediment backscatter can also be related to, or perhaps controlled by, the organisms that are living on the seabed. For example, organisms that burrow in fine-grained sediments can decrease the acoustic impedance of the seabed by creating water-filled voids unless they are tube-building organisms, which make tubes that could stiffen the sediment and thereby increase the acoustic impedance. The acoustic effects of mound-building organisms depend on the size of the mounds and whether the mounds tend to be coarser or finer than the surrounding seafloor. The burrowing can also mix any coarser surface materials into deeper sediment, and vice-versa, and thus affect the surface roughness and volume scattering. Seafloor organisms can also affect the sediment surface roughness, especially for shellfish or other organisms that have hard parts. The nature of the surface roughness and volume scattering can vary depending on the nature, size, distribution, and preservation of shelly materials. The observation that benthic organisms can alter sediment properties that affect acoustic backscatter and the observation that different groups of organisms prefer certain sediment characteristics that may control acoustic backscatter helps us understand that acoustic backscatter is an important tool in the study of benthic habitat (Cerrato et al., 2015; Flanagan et al., 2019). Indeed, studies suggest that areas with similar backscatter are likely to support a similar benthic community and that acoustic backscatter is thus an important parameter to consider when identifying the extents of different benthic communities and their habitats.

Installations

The multibeam system was installed in Port Jefferson Harbor, LI, NY, from March 3 to March 9, 2022 as part of the equipment acceptance trials with the assistance and supervision of engineers from the multibeam system vendor, Kongsberg Maritime. Following acceptance of the system, the multibeam system was used on several local projects, and on March 24 we did a short “shakedown” survey at the south end of our Phase IV (LISS) study area to gain experience using the system with this project. The “shakedown” survey was done during strong winds and with wave amplitudes over 1 m. The system worked well, although bubbles under the hull interfered with many scans, especially when going directly into the largest waves.

We utilized two vessels during three major field efforts to collect the data needed for this project. The two vessels used were the SoMAS (Stony Brook University) research vessel R/V *Seawolf* and the University of Connecticut (UCONN) research vessel R/V *Connecticut*. The Seapath and Trimble GPS antennas were installed in locations with good views of the sky, and the orientation of the Seapath antenna with respect to the vessel was determined (Figures 6 and 7). The multibeam transducer and the MRU were assembled in a frame which was then attached to the vessel. A different frame was used for each vessel (Figures 6 and 7). Both vessels have a ~0.6 m diameter tube passing through the vessel and exiting the hull (known as a moon pool).

The transducer and MRU assembly was too large to fit through the moon pool pipe, so the assembly was bolted to the base of the moon pool in a known orientation with diver assistance. Putting the transducer and motion sensor on the same frame reduces the uncertainty; knowing the distance between those two units and bolting the frame to the vessel hull ensures a stable transducer mount even at maximum ship speeds and in rough weather. The offsets between the different units, along with a measurement of the depth of the reference point below the waterline at the dock, also need to be known. The above-water components could be measured without difficulty with an estimated precision of about 0.05 m during the system installation. It was more difficult to measure the offsets to the underwater components to the antennas or to the waterline since those offsets are best measured when the boat is in drydock. We had made measurements to the underwater mounting points on the R/V *Seawolf* during previous multibeam installations while the vessel was in drydock, but we didn't have that kind of opportunity for the R/V *Connecticut*. While we thought we properly measured the locations of the underwater components on the R/V *Connecticut*, subsequent comparison with depths determined on abutting and overlapping NOAA hydrographic surveys suggest that the length we used for the moon pool pipe length was 0.25 m too short because our depth measurements made by the R/V *Connecticut* are 0.25 m shallower than the depth measurements made by the R/V *Seawolf* or by NOAA during the adjacent hydrographic surveys. We arbitrarily added 0.25 m to the R/V *Connecticut* calculated depths to make them agree with the NOAA depths. We are now waiting for an opportunity to confirm the transducer offsets on the R/V *Connecticut* when that vessel is put in drydock as part of periodic maintenance.

The multibeam system operated well on both vessels except that the transducer was not quite far enough below the hull on the R/V *Connecticut,* which somewhat affected the sonar depth record. The harbor at Avery Point where the R/V *Connecticut* is berthed is shallow and the transducer mount was designed to extend far enough beneath the hull so that the sound beams would pass beneath the keel. However, when we started to collect data, we discovered a depth anomaly of about 0.1 m on the port side at an angle of about 58 to 67 degrees from the vertical for beam numbers 19 to 73 out of a total of 400 beams. The depth anomaly probably was due to a reflection from the hull interfering with the beam forming process. This reflection did not appear to affect backscatter, and shipboard processing tests suggested that the effect of this reflection could be significantly reduced or eliminated following the cruise. So, we continued with the cruise, but so far we have been unable to fully remove this artifact in postprocessing. The depth anomaly is minimized in the final data set by using the CUBE gridding algorithm, and we are continuing to seek processing techniques that will minimize the effect of this reflection. We will continue to work on this problem, and we will submit an Addendum to the final report if we are able to make significant improvements to the data sets. The backscatter data collected during the cruise does not appear to be much affected by the hull reflection, although the processed backscatter data can show a linear feature at the site of the trough. The linear backscatter feature was apparently created during backscatter processing since that processing

can include a correction for local bottom slope. We used the R/V *Connecticut* for multibeam mapping during the unrelated Phase III project in 2023, and then the transducer was mounted 0.51 m deeper. There was no hull interference on that trip; however, the transducer mount had to be installed and removed outside of the harbor, again with diver support.

Surveys

We surveyed the Phase IV study area during cruises in August (R/V *Connecticut*), September (R/V *Seawolf*) and November-December 2022 (R/V *Seawolf*), and mapping in each area was done 24 hours/day. Our survey planning, execution and processing generally follow the guidance given in Hydrographic Survey Specifications and Deliverables (HSSD_2022.pdf and HSSD_2025-0-00.pdf ; Office of Coast Survey, 2022; 2025), available at https://nauticalcharts.noaa.gov/publications/standards-and-requirements.html. Each of our surveys consisted of a set of mostly parallel mainline tracks which covered the area, a set of tracks that crossed the mainline tracks, and a set of tracks that surveyed again a smaller area that was called the Reference Area (Figures 8, 9 and 10). The crossing tracks and the Reference Area tracks were collected to allow us to compare survey results collected on the same and different cruises so that we could determine data quality and repeatability related to our mapping technique. We surveyed another area, termed the Repeat Area, two times during the August survey where we observed a shellfish dredge operating in our study area. Data collected during stations, during turns or transits within the survey area, or when there were instrumental errors were not used to create the map products. Turns at the edges of the survey area were cropped in GIS software.

In general, the highest-quality bathymetric data is collected in the part of the swath that is closest to the ship track, and the data quality degrades somewhat at the outer parts of the swath. However, the backscatter signal tends to be very noisy near the center of the swath, and the noise levels are lower farther away from the ship track. If the objective of the survey is to get the highest-quality bathymetric data, for example during a hydrographic survey, the ship tracks should be closer together, but if the objective of the survey is to get the highest-quality backscatter data, for example during a benthic habitat study, the ship tracks can be farther apart. For this survey we prioritized the backscatter data, and we generally used a swath width of +/-70 degrees, which corresponds to a swath width to water depth ratio of 3.9:1. Our tests in March demonstrated that the bathymetric data was noisier at the outer edges of the swath, although backscatter data quality was not much affected, so we chose this swath width to maximize survey coverage while maintaining data quality. The density of depth data (e.g., depth measurements per square meter) depends on the spacing between depths in the cross-track and along-track direction. The cross-track data density depends on the swath width and number of depths determined on a swath, and the along-track data density depends on the ping rate and the ship speed. The ping rate necessarily decreases as water depth increases since the system has to wait

for the data from one ping to return before transmitting the next ping. The "dual swath" capability of our multibeam system effectively doubles the ping rate by transmitting two swaths at slightly different angles during each ping, which allows for an increased ship speed for the same data density. We were thus able to do our surveying at a ship speed of about 6 to 7 knots (3 to 3.6 m/s or 11.1 to 13 km/hr) throughout our survey area rather than slow the ship when we were in deeper water. The resulting depth data density was mostly over 50 depths/m2 for much of the survey area, increasing to mostly over 100 depths/m^2 in the shallowest waters surveyed but decreasing to mostly over 20 depths/m^2 in deeper water where we collected 256 depths/ping.

We planned a track spacing of about 3.5 times the water depth to provide enough overlap between tracks to result in 100% sonar coverage. Unfortunately, a uniform line spacing may not work well when there are along-track changes in water depth due to topography, to tides, or when an earlier survey line wasn't precisely followed due to boat traffic or other difficulties. When this occurred, the swath width was increased by the watchstander as needed to fill in a potential gap with the prior or next line so that few gaps were created. Some remaining larger gaps were filled by later gap-fill tracks. Our occasional use of a wider swath meant that the topographic data in these potential gap areas was a bit noisier, but the backscatter was not affected by the wider swath.

We mobilized the multibeam system on the R/V *Connecticut* from August 12-24, 2022, and we were assisted by an engineer from Kongsberg Maritime. During this trip we surveyed the eastern portion of the Phase IV area, here called LIS4-East (Figure 8). The weather was excellent with light winds and small waves. A minor ship problem caused the ship to return to Avery Point where the problem was quickly resolved, so our project was not charged for this equipment day.

Our main set of tracks ran primarily east-west in the southern part of the area and then switched to south-west -- north-east in the most northern part to keep the tracks running mostly parallel to the bathymetric contours. Additional tracks were run to more fully characterize Townshend Ledge and Branford Reef, which are prominent shoals in the area. We were able to run tracks across Townshend Ledge for 100% coverage, but there is not enough water on Branford Reef for the R/V *Connecticut* to pass over it. Some parts of the Connecticut shoreline in this survey area are leased for shellfish aquaculture, primarily for the depuration of shellfish recovered from inshore waters. A shellfish dredge was working in the north-west corner of this survey area during our survey, and we resurveyed an area (termed our Repeat Area) where the dredge was working in part to see if we could identify dredge marks made between our surveys.

We mobilized the multibeam system on the R/V *Seawolf* from September 6 to 16, 2022, and during this time we worked in the central part of the western portion of our Phase IV study area, map area LIS4-West-C (Figure 9). The weather was good during this survey, so we focused our work in central Long Island Sound knowing that we could work near the shore during our

survey scheduled for late November to the middle of December when the weather might be less favorable if strong winds came from the north or northwest. Our main tracks were oriented along 062-298º (NE-SW), parallel to the regional contours and we generally tried for a track spacing of less than 3.5 times water depth to reduce the number of gaps between survey lines.

Ships dredging for shellfish were encountered several times during this survey, especially during daylight hours. We avoided the dredges by working in other parts of the survey area when dredges were present to be sure that our survey operations did not interfere with the dredging activities. We defined and surveyed our Reference Area so that it overlapped with the LIS4-East survey and several long crossing lines were also surveyed. In addition to some gap fill tracks, lines using the 600 kHz option of the multibeam echosounder were collected over two specific targets, which have an uncertain origin. Additional water-column profiles using our CTD sensor were also collected near a prominent topographic feature in the south-east corner of this survey area.

Our third multibeam mobilization was on the R/V *Seawolf* from November 28 to December 8, 2022, and during this time we worked in the northern and southern parts of the western portion of our Phase IV study area, denoted LIS4-West-N and LIS4-West-S (Figure 10). While the weather was generally acceptable, there were two intense storms that passed through the area with wind speed forecast to be up to 50 mph. We returned to our dock in Port Jefferson during these events. Each storm made mapping impossible for over a day, but wave heights in the survey area decreased to an acceptable level once the winds subsided due to the limited fetch in Long Island Sound.

Our main survey tracks continued to follow the 062-298 º orientation. Data in the northern and southern portions collected on this cruise were processed separately since the survey grids do not overlap. We ran crosslines that crossed both the September and the November-December data, and we collected a new set of tracks in the Reference Area defined during our September survey. In addition, some additional lines were run in areas of interesting topography in the southern portion of the area, and two transects of CTD profiles were collected in the southern area.

For this survey, the multibeam swath was set so that 256 depths were determined across the swath rather than the 400 depths determined for the two prior mobilizations to evaluate how this setting affected the survey results. While the spacing between depth in both modes was adequate to create depth grids with a 1 m cell size, the outermost portions of the depth swath appeared to be somewhat less noisy for the 256 depths setting than for the 400 depths setting. Also, the backscatter levels obtained after processing with CARIS HIPS and SIPS software was about 7 to 10 dB lower for the 256 depths setting than for the 400 depths setting. To correct for this offset in backscatter intensity, 7.0 dB was added to the backscatter grid for the LIS4-West-N

survey and 10.5 dB Was added to the backscatter grid for the LIS4-West-S survey to make the values more closely agree with the LIS4-West-C and LIS4-East surveys.

The processed data grids for the four individual surveys were combined to create single files with a resolution of 1 m for bathymetry (water depth), backscatter, and two directions of hillshade images (Figures 11-15) using the ArcGIS Pro geoprocessing tool Mosaic to New Raster. The naming template is LIS4_<data type>_<horizontal datum>_<resolution>. The vertical datum for the water depth data is NAVD-88 and the horizontal datum for all grids is NAD83(2011). The ArcGIS Pro Aggregate tool was used to create reduced-resolution files with grid sizes of 2 m and 5 m, and all files were saved in GeoTIFF format suitable for importing into GIS software.

The names of the merged files are as follows:

Bathymetry:

LIS4_Depth-NAVD88_NAD83_1m.tif
LIS4_Depth-NAVD88_NAD83_2m.tif
LIS4_Depth-NAVD88_NAD83_5m.tif

Backscatter:

LIS4_Backscatter_NAD83_1m.tif
LIS4_Backscatter_NAD83_2m.tif
LIS4_Backscatter_NAD83_5m.tif

NW-Hillshade:

LIS4_NW-Hillshade_NAD83_1m.tif
LIS4_NW-Hillshade_NAD83_2m.tif
LIS4_NW-Hillshade_NAD83_5m.tif

NE-Hillshade:

LIS4_NE-Hillshade_NAD83_1m.tif
LIS4_NE-Hillshade_NAD83_2m.tif
LIS4_NE-Hillshade_NAD83_5m.tif

These files, along with appropriate metadata, are being submitted for archiving to the to the LIS Data Portal on the Marine Geoscience Data System (https://www.marine-geo.org/collections/#!/collection/LIS#summary). Current requirements for submitting hydrographic survey data to NOAA NCEI are given in https://www.ncei.noaa.gov/iho-data-centre-digital-bathymetry/submitting-marine-geophysical-data and are being reviewed. The

anticipated name of the data set is: "Long Island Sound Study (LISS) Phase IV 2002 Multibeam Mapping south of New Haven, CT, 2022, SoMAS, Stony Brook University."

Bathymetric Data Comparisons

The accuracy and repeatability of our depth data was evaluated through comparing gridded bathymetric data sets collected during different surveys or at different times in ArcGIS Pro. The depth data sets being compared are the survey crosslines, the resurveyed areas, the primary depth data, and depths in adjacent NOAA survey areas. These comparisons were important for determining if the depth data was properly corrected for instrumental offsets, sound velocity variations, and water level. While no formal requirement for Total Vertical Uncertainty (TVU) was defined for this survey, the statistics calculated for our data set comparisons can be used as part of an evaluation of TVU.

The document HSSD_2025-0-00.pdf (Office of Coast Survey, 2025) states that the maximum allowable Total Vertical Uncertainty for a hydrographic survey is defined as

$$TVU_{max}(d) = a + (b \times d)$$

Where:

a represents the portion of the uncertainty that does not vary with depth
b is the coefficient which represents that portion of the uncertainty that varies with depth
d is the depth.
b × d is the portion of the uncertainty that varies with depth.

While the vertical uncertainty for a particular survey is related to many factors including the survey equipment, the equipment installation, oceanographic conditions, and weather conditions at the time of the survey, one useful characterization of the vertical uncertainty for a survey comes from the comparison of water depths determined where crossing lines intersect the main survey lines, where different surveys overlap, and where the current survey data overlaps prior surveys conducted in the area. Office of Coast Survey (2025) states that the maximum allowable TVU value for a survey meeting an OCS Quality Metric of "Exceptional" is 0.15 m, an OCS Quality Matrix of "Critical" is 0.25 m, and an OCS Quality Matric of "General 1" is 0.5 m (i.e., a = 0.15 m, 0.25 m and 0.5 m respectively). TVU estimates need to be met at the 95% confidence level.

As noted before, there was a consistent 0.25 m offset between the R/V *Connecticut* surveys and both the R/V *Seawolf* and adjacent NOAA multibeam hydrographic surveys. This offset is most likely due to an error in the length of the R/V *Connecticut* moon pool pipe. We are seeking verification of this offset, which might not be measured until the R/V *Connecticut* is taken out of the water for routine maintenance. For the comparisons described here, a depth offset of 0.25 m has been added to the R/V *Connecticut* depth data (LIS4-East survey), which

makes that data set consistent with the other depth data in the region collected by this project and by NOAA.

Our comparisons show that there is good agreement within each of the data sets, between data sets, and with the adjacent NOAA multibeam hydrographic surveys for the surveys done during this project (Figure 16). The calculations were made using project (LIS4) survey data gridded at 1 m and data for adjacent surveys gridded at 2 m. If the distribution of depth errors follows a Gaussian distribution, around 68% of the depth comparisons are expected to be within 1 standard deviation of the mean, around 95% of the depth comparisons are expected to be within 2 standard deviations of the mean and 99.7% of the depth comparisons are expected to be within 3 standard deviations of the mean. The mean value +/- 2 standard deviations for nearly all of the LIS4 depth comparisons and comparisons between the LIS4 and adjacent NOAA multibeam hydrographic surveys fall in the range of +/- 0.25 m suggesting that the LIS4 depth data will meet most of the requirements for a "Critical" depth survey.

Phase IV Survey-Crossline Comparisons

Both the main survey tracks and the crossing survey tracks for each survey area were gridded at a 1 m resolution, and the grids for the main tracks and the tracks that crossed those areas were compared in ArcGIS Pro. Only the central portions of the crossing tracks were used for this comparison to reduce errors related to incorrect refraction corrections. We expect the offsets to be small if the water-level records used to process the data files are consistent and refraction corrections have been made. The mean values of the eight survey depth comparisons (four comparisons within surveys and four comparisons between surveys) range from 0.014 m to 0.131 m, and the standard deviations go from 0.039 m to 0.079 m. The largest mean offset (0.131 m) occurs between West-C (September, 2022) and West-S (November-December, 2022) data sets which might be because we did not account for fuel usage or refueling during these surveys.

Phase IV Resurveyed Area Comparisons

Two resurveyed areas were defined. Data was collected in the Reference Area during all three surveys, and data was collected in the Repeat Area only during the LIS4-East survey area (R/V *Connecticut*). The three grids for the Reference Area were compared two at a time. The mean depth offsets ranged from -0.050 m to 0.018 m with standard deviations ranging from 0.037 m to 0.064 m. The two data sets from the Repeat Area in the August survey (LIS4-East) had a mean difference of 0.018 m and a standard deviation of 0.038 m.

Phase IV Survey Overlap Comparisons

Our four primary survey areas (LIS4-East, LIS4-West-C, LIS4-West-N and LIS4-West-S) overlap to a limited extent and depth offsets can be calculated for the overlap areas. The mean offsets in the overlapping areas range from -0.114 m to 0.068 m with standard deviations ranging from 0.035 m to 0.058 m. Again, the largest mean offset (-0.114 m) occurs between West-C (September, 2022) and West-S (November-December, 2022) data sets which might be because we did not account for fuel usage or refueling during these surveys.

Phase IV Survey and NOAA Survey Comparisons

The Phase IV study area lies adjacent to seven NOAA/NOS hydrographic survey areas, which were mapped with 100% coverage by multibeam techniques in 2012 and 2013 (Figure 17). The adjacent hydrographic surveys are H12417, H12437, H12438, H12479, H12480, H12481 and H12485, and more information about and data from these surveys can be found at https://www.ncei.noaa.gov/maps/bathymetry/. An additional survey (H13929) was conducted in 2024 that overlaps the West-S survey area and that survey data is also used for this comparison. The NOAA survey results are reported with respect to the MLLW hydrographic datum and the software package VDatum (https://vdatum.noaa.gov/) was used to convert the NOAA survey results to the NAVD88 vertical datum. The depth grids provided by NOAA have a 2 m grid cell, whereas our Phase IV survey grids have a 1 m grid cell. Differences were calculated between each of the Phase IV grid areas and an overlapping NOAA survey.

The mean offsets between data from the R/V *Seawolf* surveys and adjacent NOAA surveys range from -0.043 m to 0.086 m, and standard deviations range from 0.077 m to 0.120 m. The mean and standard deviations are 0.054 m and 0.097 m when all the R/V *Seawolf* and the NOAA hydrographic survey data are evaluated together. The mean offsets between data from the R/V *Connecticut*, after a correction is made for our likely 0.25 m depth error, and an adjacent NOAA survey range from -0.042 m to 0.022 m and standard deviations range from 0.054 m to 0.110 m. The mean and standard deviations are -0.003 m and 0.101 m when all the R/V *Connecticut* and the NOAA hydrographic survey data are evaluated together.

For comparison purposes, the seven NOAA hydrographic surveys that overlap with our Phase IV surveys themselves overlap in six areas. The mean offsets between adjacent surveys (not including the most recent survey H13929) range from 0.007 m to 0.049 m with standard deviations ranging from 0.033 m to 0.138 m. These overlaps are in the general range of the overlaps calculated using the Phase IV survey data.

Depth comparisons are also made between our Phase IV depth grids and prior NOAA surveys H11001 (conducted in 2000), H11043 (conducted in 2001) and H11044 (conducted in 2001). While multibeam sonar was used to collect some or all of the bathymetric data in these surveys, the survey results are only reported as point depths in x, y, z format rather than depth

grids with 100% coverage. We gridded these survey data resolutions of 10 m, 15 m, and 30 m, respectively, to provide a fully populated grid that could be compared with the Phase IV multibeam data although the large grid size is expected to induce errors into the hydrographic survey results. The gridded NOAA depths were converted from the MLLW datum to the NAVD88 datum using VDatum. H11001 and H11043 primarily overlap with the LIS4-East survey set while the H11044 survey data primarily overlap with the LIS4-West surveys. The mean offset for surveys H11001, H11043 and H11044 are -0.113 m, -0.251 m and -0.268 m and the standard deviations are 0.159 m, 0.230 m and 0.246 m, respectively.

The Phase IV survey area lies adjacent to the LISPilot area studied by the LIS Seafloor Habitat Mapping Initiative in 2014. The bathymetric survey for the area was collected by NOAA surveys H12416 and H12417 and by SoMAS surveys done on the R/V *Seawolf* and the R/V *Pritchard*. The results of the four SoMAS LISPilot surveys and two NOAA hydrographic surveys were combined by NOAA and were published as NCEI Accession 167946 (Battista et al., 2017). The Phase IV and the combined LISPilot depth data, with vertical datum of NAVD88, have a mean offset of 0.005 m with a standard deviation of 0.151 m.

Backscatter Data Comparisons

Backscatter data values were compared where the Reference Areas, Repeat Areas, and the main surveys areas overlapped. No backscatter comparisons were made with the crosslines or could be made with adjacent NOAA survey areas since the NOAA survey data is scaled between 0 and 255 rather than reported in dB units (Figure 18). As noted previously, backscatter comparisons between the different surveys show that the backscatter levels in the LIS4-East and LIS4-West-C (R/V *Connecticut* and R/V *Seawolf* in September) surveys were consistent but differed from the backscatter levels in the LIS4-West-N and LIS4-West-S (R/V *Seawolf* in November-December) surveys. The R/V *Seawolf* survey in November-December collected 256 depth values per swath rather than 400 depth values per swath, and it is likely that the different backscatter levels are due to that change. The backscatter levels for the different surveys can be made consistent by adding 7 dB to the backscatter levels in the northern part of the November-December survey area and 10.5 dB to the backscatter levels in the southern part of the survey area. The value of 7 dB comes from comparing values from LIS4-East, LIS4-West-C and LIS4-West-N, including in the Repeat Area, and the value of 10.5 dB comes from comparing LIS4-West-C and LIS4-West-S where there is only a small overlap. The comparison described below includes these backscatter offsets.

Backscatter data was collected in the Reference Area during all three surveys, and data was collected in the Repeat Area only during the LIS4-East survey area (R/V *Connecticut*). The three grids created for the Reference Area were compared taken two at a time. The mean backscatter offsets ranged from -0.522 dB to 0.074 dB with standard deviations ranging from

0.784 dB to 0.916 dB. The two data sets from the second reference area in the August survey (LIS4-East) had a mean difference of 0.270 dB and a standard deviation of 0.593 dB. Backscatter values can be compared in four areas where the main surveys overlap. Mean offsets range from 0.017 dB to 0.390 dB, and standard deviations range from 0.628 dB to 0.899 dB.

Survey Results

Our multibeam survey activities and processing steps have resulted in high-resolution bathymetry and backscatter datasets, which, along with other datasets, will be important to characterizing and understanding the benthic habitat in the Phase IV Study Area of the Long Island Sound Cable Fund Seafloor Habitat Mapping Initiative. These datasets will provide a wealth of information about the character of the seabed, the processes that have formed and that continue to modify the seabed, and the substrate that supports the benthic populations in Long Island Sound. Preliminary versions of this multibeam data set have been used by others to plan recent and future studies as part of the overall Phase IV study. Some preliminary results of those recent studies are available which can help to interpret these results. Samples and seabed imaging studies have also been done by others in past years which also help us to understand the significance of our current studies. Many of the recent studies have been summarized in Latimer et al. (2014) and grain size measurements made during those and other studies are available at usSEABED (Buczkowski et al., 2020 and elsewhere). In addition to NOAA hydrographic studies mentioned earlier, USGS has published at least several open-file reports describing side-scan sonar data and sediment samples collected in conjunction with NOAA hydrographic studies (Poppe et al., 2004; McMullen et al., 2005; McMullen et al., 2008). Frank Nitsche (LDEO, personal communication, 2024) also provided preliminary results about grab samples collected in 2023 as part of the LDEO Phase IV studies. This report will refer to prior data where it helps to understand the current multibeam dataset. We expect to have a better understanding of the Phase IV mapping data as results become available during the ongoing Phase IV studies.

In this report we will first compare in some detail the bathymetric and backscatter data collected in the Reference Area and the Repeat Area as a way of describing the nature, quality and repeatability of the survey data. Then we will make a general description of the multibeam survey results throughout the Phase IV area, integrating where possible existing data as well as preliminary data collected by others as part of the ongoing Phase IV studies. Finally we will highlight some particularly interesting survey results which may help us to understand the complexity and evolution of the seafloor in this region.

Reference and Repeat Areas

Comparing results of the different surveys in the two areas that were resurveyed gives some insights into the quality of the multibeam data and the nature of the seabed in those areas as well as provides some general guidance about interpreting these multibeam data sets. Locations of the Reference Area and Repeat Area are shown on Figure 19 and the mapping results are shown in Appendix A, Figures A1-A5, on three panels per page. The top panel image is hillshade bathymetry illuminated from the northwest, the middle panel image is hillshade bathymetry illuminated from the northeast and the bottom panel image is backscatter. Available sediment samples suggest that sediments in the Reference Area are muds and muddy sands while available sediments in the Repeat Area are mostly sands and sandy muds with finer grained sediments present closer to and in the dredged channel.

The Reference Area was surveyed three times, in August, September and November-December (Figures A1, A2 and A3). The two hillshade images from August (Figure A1 top and center) clearly show the slight depression on the outer edge of the port side, especially where the port sides overlap, while little striping due to that depression is seen on the backscatter image (Figure A1, bottom). There is no similar depression on the hillshade images from September or November-December (Figures A2 and A3, top and center) although some noise in the depth data is present at the outer edges of the swaths, especially in the November-December data (Figure A3, top and center). There was less ship motion in September (roll +/- 0.5º, pitch +/- 0.25º and heave +/- 0.02 m) than in November-December (roll +/- 2º, pitch +/- 1º and heave +/- 0.2 m). Quite small topographic features such as troughs, mounds and pits can be observed on the hillshade images for all three surveys and their locations and character are similar on all surveys although features are less distinctive when they are aligned with the sun illumination direction. In particular, the hillshade images show many slightly elongated depressions which have diameters of about 5 m to 10 m and depths of only 0.1 m to 0.2 m. These shallow depressions appear quite prominent because of the large vertical exaggeration used to create the hillshade images. At least three shallow, linear depressions are seen with lengths of 100 m or more and which may have been formed when equipment was dragged on the sea floor.

The backscatter data from the Reference Area shown on the bottom images of Figures A1, A2 and A3 is similar in pattern and in value on all surveys. There is some slight east-west striping in November-December data (Figure A3, bottom) which is along the center of the swath. The increased striping there may result from measuring 256 depths per ping rather than 400 depths per ping during that survey. Also, there are some faint, whispy darker areas in the upper-right quadrant of the backscatter images of Figures A1 and A4. These whispy areas are caused by fish in the water column scattering and attenuate sound so that their backscatter levels are lower. The echoes from fish are sometimes recorded as shallow depths in the depth data and careful cleaning of the bathymetric data is needed to remove those spurious depths.

Figures A4 and A5 show hillshade and backscatter imagery collected in part of the Repeat Area that was surveyed in August. The small, along-track grooves at the outer edge on the port side can be seen in Figures A4 and A5 but they are less distinct than in the resurvey data shown in Figures A1 to A4. This is because the tracks were relatively closer together in the Repeat Area than in the Reference Area. Slight vertical offsets can be observed between adjacent tracks on several of the hillshade images where the water-level records and/or refraction corrections used in processing the depth data have some inconsistencies. The hillshade images of Figures A4 and A5 show the loopy tracks of a shellfish dredge as it moves across the seabed. The State of Connecticut leases the seabed in Long Island Sound for aquaculture purposes and these dredge tracks are apparently the result of that activity. Shellfish recently harvested from uncertified grounds in Connecticut estuaries are transplanted to these leased areas for depuration in the clean Sound waters. The shellfish are recovered by later dredging and sold, and the tracks seen here were created during the recovery of the shellfish. In addition to the loopy dredge tracks, numerous smaller ridges can be observed, especially in areas with no or few dredge tracks. Prior work in the LIS Cable Fund Seafloor Habitat Mapping Initiative has suggested that smaller ridges like these may be strings of mussels. These probable mussel strings are not commonly observed where there are shellfish dredging tracks, which is interesting.

The backscatter images in the two surveys shown in the Repeat Area (Figures A4 and A5) are quite similar, although there is some weak along-track striping that may occur along the depth artifact present on the port side and along the center of the swath. The depth data in Figures A4 and A5 shows a near-circular depression that is about 50 m across and 1.5 m deep in the southeast part of Figures A4 and A5. The floor of this depression has low backscatter which may suggest that fine-grained sediments have been accumulating in the depression. However, a sample possibly taken in this depression in 1968, before precise navigation was available, shows a sandy sediment and fine sands can also have low backscatter. Another small area with low backscatter can also be observed to the east of the depression, but no topographic depression is present there. On close inspection of the backscatter images one can see that there are light or white tails of seabed with apparently higher backscatter (lighter color) extending along track both east and west of the low-backscatter features. These tails are likely artifacts of the backscatter processing which is trying to smooth out, or average out, along-track intensity variations. When the along-track averaging window includes a patch of low-reflectivity seafloor, the algorithm increases the gain. The increased gain amplifies the backscatter data adjacent to the patch of low backscatter which results in a higher signal level (lighter color) adjacent to the low backscatter patch. This happens on both sides of the patch of low backscatter patch. Thus we end up with a patch of low backscatter (darker color) with tails of higher backscatter (lighter color) on either side. There is no higher-backscatter material on the seabed on either side of the low backscatter patch; these lighter tails are artifacts of the processing algorithm. While the processing software used for this study had fewer of these kinds of artifacts than did other

software programs we experimented with, this phenomenon needs to be considered when interpreting the backscatter data.

The backscatter data shown in the lowermost panels of A4 and A5 show thin, long and often curved strings of low backscatter, which align with some of the dredge tracks in the hillshade images. These thin areas of low backscatter material may be due to fine-grained sediments that accumulate in the depressions formed by the dredging. With time, older dredge tracks fill and any fine-grained material is buried by transported sediment and/or mixed into coarser sediment by biological activity.

The Phase IV Survey Area

The Phase IV study area is located offshore of New Haven, CT, and extends about 28 km along the Connecticut shoreline from Branford, CT, on the east to Milford, CT, on the west. The nearshore limit of the study area is about the 8 m depth contour, which ranges from 0.5 km to 3 km offshore. West of New Haven the area extends up to 23.5 km from the Connecticut shoreline, which is about 5.5 km from the New York shoreline at Rocky Point, NY. South and east of New Haven the area extends to about 11 km offshore. The depths measured during the surveyed range from about 5 m near Branford Reef to over 47 m near the southern end of the survey area.

The morphology in the northern part of the study area, up to about 13 km offshore, consists of a gently sloping seabed (about 0.09º) to a depth of about 25 m. This gentle slope is interrupted by two smoothed rises perpendicular to the shoreline with heights of about 1 to over 3 m and widths of up to about 3 km. A third similar ridge that doesn't extend as far offshore is present just east of New Haven. The rises are located near Milford Harbor, offshore of Welches Point and Pond Point, and just west and east of the entrance to New Haven harbor. The rises extend offshore to a depth of about 20 m off Milford and depths of about 15 m off New Haven. Arcuate ridges extend to the sides of these rises, especially in water depths shallower than about 15 m, although arcuate ridges can be identified in deeper water. These rises have distinctly higher backscatter and the areas between the rises generally have lower backscatter. This is consistent with sediment samples, which show that the surface sediments of the rises are often sand-sized and coarser while the sediments between the rises are finer, almost exclusively described as muds. One likely explanation of the rises is that they formed as the post-glacial rise of sea level flooded the depression of Long Island Sound and eroded headlands, and the retreating headlands left a trail of coarser sediments on the seabed. The arcuate ridges may have formed as shoreline deposits near headlands during that sea level rise and then were abandoned as sea level continued to rise. Currents continued to rework bottom sediments on these rises as sea level rose, continuing to today, and sediments eroded from the rises will likely be found in the areas of intermediate backscatter levels often observed within about 500 m of the rises.

Two small apparent rocky features were mapped east of New Haven. Townshend Ledge rises about 7 m above the seabed to a water depth of less than 8 m while Branford Reef rises from a water depth of about 11.5 m to a water depth of perhaps 1 m (we did not survey on top of Branford Reef). There are significant sediment tails and scoured areas near both Townshend Ledge and Branford Reef, and the scoured depression on the north side of Branford Reef is very deep, reaching a depth of 26.4 m (over 25 m deeper than the adjacent reef). The scoured depression on the south side of Branford Reef reaches a depth of 17.6 m. Several other small areas with likely rock outcrops have also been identified in this general area. Some of these are marked as rocks on the chart, and some are not.

The western-most of the offshore trending rises appears to continue into deeper water to about 30 m water depth as a topographic and high-backscatter feature, although the trend of the feature may change slightly at a water depth of 20 to 22 m. This deeper rise has a height of about 1 to 2 m and width of about 2 km, and the western side of the rise at the deeper end is somewhat steeper than the eastern side. The rise extension also has higher backscatter than the surrounding seabed, although sediment samples suggest that sediments on the rise is getting finer in deeper water. Deeper than 24 m, the western side of the rise is distinctly steeper than the eastern side with a slope locally over 2º. Also, a distinct depression at the base of the slope is about 1 m deep, 200-300 m wide and parallel to the steeper western side of the rise. This deeper rise goes out our Phase IV study area and was also mapped during NOAA surveys H12438 and H12481 (Figures 17 and 18). Our Phase IV study area was extended slightly to the east to ensure that it overlapped part of this distinctive feature.

The topographic rise just west of New Haven doesn't extend deeper than about 20 m as a topographic feature. There are many mounds and areas of higher backscatter there deeper than 20 m, but most of that material appears to be dredge spoils. Indeed, this area is labeled "Dumping Ground (dredged material)" on NOAA nautical chart 12354. A portion of the dumping ground was mapped during NOAA survey H12481. The chart also designates two anchorages in this general area and many of the high-backscatter areas in these areas may be related to sediment disturbances related to vessel anchoring (McMullen et al., 2005).

A distinctive, irregular area that rises about 5 m above the seafloor is observed at water depths of 30 m to 35 m at the south end of the Phase IV study area. This feature is informally named "Bunny Rise." The rise roughly has a diamond or triangular shape with the longer, north-south direction being 5 km and the shorter, east-west direction being 3 km. Like the other rises, the west-facing edge of the rise is considerably steeper than the other rise edges with slopes sometimes about 3º and there is a distinct depression running parallel to the scarp is found at the base of the west-facing slope.

This central LIS deep-water rise is presently somewhat isolated but a topographic feature at a similar depth on the north-facing slope of Long Island may have connected to the central LIS rise in glacial or early post-glacial times to form a 10 km long rise extended northward into Long Island Sound (Figure 20). The central part of this earlier rise appears to have been eroded and now there is a 3 km wide, 10 m deep gap in this earlier rise. That gap probably was created during early post-glacial times when the floor of Long Island Sound was dry land and a river flowed toward the east along the deep axis of the depression. The hillshade imagery of the base of this depression reveals what appears to be a meandering channel at a water depth about 40 m, and parts of that channel can be followed for at least 13 km in the west-east direction (Figure 20). The channel appears to be completely buried going east where the depth is shallower than about 40, and the channel appears to have been removed later by erosion towards the west where the depth is deeper than about 41 m. Nearly all present-day sediment samples report muds, but some there are some coarser samples. If the channel has cut through the deep-water rise, then the rise was formed before the channel, which suggests a possible late glacial/early interglacial age for the rise or perhaps formation during an earlier glaciation. Other topographic rises with high backscatter are also found to the east and west of the Phase IV study area, but outside of the Phase IV study area, which may also have been deposits that pre-date this ancient, post-glacial drainage system.

Long Island and Long Island Sound are located at or near the southern terminus of repeated major continental ice sheets that formed in North America from about ~781,000 to 18,100 years ago (Lewis and Stone, 1991; Uchupi et al., 1999; Lewis, 2014). During that time, enough of the water on the Earth's surface was incorporated into glaciers to lower the water surface of the ocean about 100 meters. At that time, much of the present-day continental shelf, including the continental shelf south of Long Island, was exposed dry land, and the shoreline was near the present-day 100 m isobath. The immense weight of the ice sheet also loaded the continental crust, causing the land to subside beneath the ice and near the ice edge (Peltier, 1998). The global ice sheets started melting about 18,000 years ago, and meltwater flowing into the ocean resulted in a rapid sea level rise to about 6,000 years ago. Mountain glaciers and continental ice sheets in Greenland and Antarctica have melted at a lower rate since then, and sea level has continued to rise to its current level. It is likely that sea level will continue to rise as more land-based ice melts.

The land of Long Island was in part shaped by the activity of the continental glacier since the edge of the glacier was at about Long Island, and the glacial moraines that make up Long Island were deposited at the edge of the glacier. Glacial activity also created a large trough north of Long Island which is the present-day location of Long Island Sound (Lewis and Stone, 1991; Uchupi et al., 1999; Lewis, 2014). The glacier that formed Long Island also apparently deposited a moraine across the east end of present-day Long Island Sound that trapped glacial meltwater as the glacier retreated creating a large lake now known as Lake Connecticut. This

lake apparently started forming about 18,000 years ago. The morainal deposits that dammed Lake Connecticut were inherently unstable and the dam failed about 15,000 years ago causing Lake Connecticut to start to drain. After draining, the floor of present-day Long Island Sound (the former Lake Connecticut) was dry land, and water from upriver sources created a river that flowed through that depression and continued across the shelf to the shoreline. When it was active, that river encountered a rise of uncertain origin, the 10-km long north-south rise described above, that blocked the course of the river. Eventually the river cut down, eroding a pathway across the rise and creating the abandoned river bed we see now. Sea level continued to rise as the glaciers continued to melt, and about 12,400 years ago, ocean waters got high enough to enter and create Long Island Sound. Sediment has accumulated in the area, burying the channel with more recent sediment to the east and south. However, current flow in Long Island Sound seems to have been sufficient to restrict sediment deposition along portions of the reach of channel we see today. The relict, meandering channel that we observed at a depth of about 40 m is, thus, probably a remnant of that early interglacial river channel that was active after Lake Connecticut drained until the rising sea level entered and created Long Island Sound. The sea level history in this area is made somewhat more complicated by the fact that the immense weight of the ice sheet depressed the land during glacial times, and the land rebounded (i.e., became higher) once the weight of the ice was removed (Peltier, 1998). If indigenous peoples were living in this area at that time, it is possible that they visited this river when this was dry land. However, the history of indigenous peoples in this area is poorly known, in part because some of the areas that they would have inhabited are now underwater.

Natural Features that Characterize the Phase IV Area

In addition to the overall characteristics of the Phase IV study area described above, there are many features that provide important insights into the natural processes active in the area. This section describes and illustrates a variety of features and provides some references, but much more can be written than is appropriate in this report.

It is recognized that bottom currents are important agents in resuspending, transporting and depositing sediment in Long Island Sound and that tidal bottom currents and storm waves and currents are important to sediment distribution patterns in Long Island Sound (Bokuniewicz and Gordon, 1980; Signell et al., 2000; O'Donnell et al., 2014). The results of our study support the suggestion that the generally smooth seafloor in the Phase IV area is due to the action of tidal currents and storm waves and currents in Long Island Sound. Poppe et al. (2002) used side-scan sonar data collected during NOAA hydrographic survey H11043 in the eastern part of our LIS4-East survey area to note that sedimentary furrows were common in this area. Our results support this observation (Figure 21; water depth 22 m). Sedimentary furrows are linear grooves in the seafloor in fine-grained sediments that are aligned parallel to current flow (Flood, 1983), and they can characterize depositional or intermittently erosional areas with persistent,

directionally stable flows. In the Phase IV area furrows are found in water deeper than about 19 m in the area east of New Haven. The furrow field extends out of our study area to the east and to the south, although furrows are also found in the Phase IV area at the western part of our study area at depths of about 28 m to 33 m. The furrows here range in depth from about 0.1 m to 0.6 m, have widths of about 5 to 10 m, and can extend a km or more in the along-current direction. The backscatter of the furrowed sediments is quite uniform, although possibly higher backscatter in the troughs of the larger furrows suggest that the sediments there may be a bit coarser.

The Central Long Island Sound Dredged Material Disposal Site (CMDS; https://www.epa.gov/ocean-dumping/dredged-material-management-long-island-sound#Central%20and%20Western%20ODMDS) overlaps the eastern portion of the Phase IV survey area. The disposal of clean, generally fine-grained sediment that has greater than 20 to 40% fine content and has been determined to be suitable for open-water placement can be permitted in the CMDS. A number of deposits that are likely to be dredge spoil deposits were identified in the CDMS and the deposits shown in Figure 22 (water depth 20 m) have heights up to 0.5 m, diameters up to 100 to 150 m and possibly elongated towards the west. Materials that are dropped on the seabed, such as the dredge spoils, often create either a circular, crater-like feature on the seabed or a conical feature, perhaps with a flat top. Both of these morphologies are present here. The seabed areas next to the dredge spoil deposits have a furrowed topography and the furrows seem to cross and locally erode these dredge spoil deposits. This area of the seafloor was surveyed during NOAA hydrographic H11043 done in 2001 (McMullen et al., 2008; Figure 23), and that survey appears to show fewer mounds, perhaps only one cluster of deposits, as well as a furrowed seabed where there are now dredge spoil mounds. This suggests that the mounds have been somewhat modified by currents in the last 20 or so years.

As noted above, much of the seabed in the Phase IV study seems to have a smoothed character, perhaps smoothed by persistent tidal currents (Figure 24; water depth 15 m). However, in some areas deeper than about 13 m there are also numerous pits with depths of about 0.2 m to 0.5 m and diameters of about 20 m to 50 m. The floors of the pits appear to be flat with diameters of about 5 m to 10 m and higher backscatter. The walls of the pits have gentle slopes, generally less than 2º, and so may be difficult to identify on the seafloor. The pits appear to occur in lines with lengths of a few hundred meters to perhaps one kilometer. The pits are similar in character to pockmarks that have been linked by many to occasional fluid or possibly gas discharges which may be important in creating seafloor heterogeneity (Sánchez et al., 2021). Some other arcuate depressions are also seen in this area, also with depths of about 0.2 m to 0.5 m, and there is a distinct, linear feature with a similar depth that crosses the figure from east to west. This linear feature was likely made as an anchor or other gear was dragged across the seabed by a vessel.

There are few possible rocky areas in Phase IV study area and most of the areas identified are east of New Haven. The two most prominent features are Branford Reef and Townshend Ledge (Figure 25), which rises 7 m above the adjacent seafloor to a water depth of 8 m. Townshend Ledge has high but apparently variable backscatter, and a region of higher backscatter extends on the flatter seafloor for about 200 m from the pronounced topographic feature.

Some more complex interactions are observed between topography and the currents that flow at depth in Long Island Sound (Figure 26; water depth 28 m to the west, 26 m to the east, 30 m in base of trough) where a 2 m deep, rounded depression is found on the west side of a 4 m high scarp. Short furrows appear to form in the trough, and the spacing between the furrows increases to the west as some furrows die out. This pattern is consistent with a weakly stratified flow flowing from east to west across the top of the scarp, accelerating down the 2º west-facing slope and then slowing as the flow encounters the western edge of the trough. The furrows are found where the accelerated flow is strong enough to cause some erosion in the furrows, and the generally stronger flow in the trough reduces deposition and keeps the trough from filling. The phenomenon is similar to the lee waves formed by air flow over mountains (see for example Durran, 1986) and such flows are known to occur in the deep sea and affect sediment deposition patterns (e.g., Flood, 1988). Similar scarps with one or more parallel, rounded topographic ridges west of the scarps are found in other nearby areas in Long Island Sound (see Figure 20).

Figure 26 also shows the presence of nearly north-south trending, somewhat sinuous troughs with lengths up to about 400 m, variable widths up to about 15 m and depths of about 0.2 m to 0.5 m. The floors of the trough also tend to have backscatter that is higher than the surrounding sediments. Features similar to these are found in many parts of the Phase IV study area where there are fine-grained (low backscatter) sediments. There is some morphological similarity between the lines of pits observed in Figure 24 and these somewhat sinuous troughs suggesting that the troughs can evolve into lines of pits over time. The existence of the somewhat sinuous troughs may be related to the thick sediment sequence of rapidly deposited, fine-grained glacial lake and earlier sediments over 10 m thick thought to exist beneath the modern sediments in parts of Long Island Sound (Lewis and Stone, 1991; Lewis and Diagiacomo-Cohen, 2000). Such deposits dewater and compact over time, and Cartwright and Lonergan (1996) suggest that polygonal faulting systems that extend over large areas can develop in those conditions. The horizontal scales of the faulting can be on the order of several hundred meters and, thus, be similar to the scale of the irregular troughs seen here. Cartwright et al. (2004) demonstrate the existence of similar faulting in thick, fine-grained sediments of glacial origin that underlie Lake Superior, and they relate the faulting to pockmarks observed in the subsurface. Flood and Johnson (1984) described seabed features called “rings” in Lake Superior that are quite similar to the sinuous troughs described here on the basis of side-scan sonar records, and Cartwright et al. (2004) suggest that their pockmarks and the rings may be

genetically linked. The somewhat sinuous troughs described here have a preferred nearly north-south orientation, which might occur if the thick, fine-grained fill has a larger east-west extent and a more limited north-south extent.

The morphology of Bunny Rise, the deep-water topographic feature described earlier, has characteristics that appear to be related to the history of the deposit and the local sedimentary processes (Figure 27). The modern deposit has a complex backscatter pattern, which is likely to represent one or more important benthic habitats since they are coarser sediment deposits in deep water that are several meters above the local seafloor. The top of the rise is fairly flat with a width of about 600 m and depth of about 25 m in the north, increasing to 2 km or more in width and a depth of about 30 m in the south. There are a few topographic features on the rise with heights of about 0.5 m, which may be outcrops of the underlying sediment. Grab sediment samples show sand, muddy sand and sandy mud, and mostly mud. There is a distinct, rounded depression and ridge system on the west side of the northern rise which, like in the case of Figure 26, may be due to a westward flowing stratified flow spilling down the west side of the rise. Several other similar trough and ridge systems appear on the west side of a smaller rise in the southwest corner of Figure 27. There are some short (100 m to 300 m long) furrow-like linear troughs immediately to the east side of the rise, which all seem to have been initiated by flow around an obstacle on the seafloor. The short extent of the troughs may indicate that the strongest flows here are mostly tidal and the flow disturbance created by the obstacle does not continue far away from the obstacle. Longer furrows, likely related to steadier, westward current flow, appear at the eastern edge of the figure. The backscatter image shows low backscatter on either side of the rise where samples are primarily muds and intermediate and high backscatter values close to and on the rise where samples have some sand component. Some of the local peaks have the highest backscatter in the area but the steep, west-facing slopes also can have high backscatter. The wispy higher backscatter pattern found east and west of the rise are likely due to coarser sediments being carried of the rise by bottom current flow. The north-south sinuous troughs are mostly filled near the rise. Also, while not visible at the scale of Figure 27, a cable that goes from Wading River, NY, to Connecticut crosses the eastern portion of Bunny Rise. The trough for that cable can be seen in some areas but it is filled in other areas.

The meandering river channel described earlier is imaged in higher resolution in Figure 28. The channel here is in a water depth of 41 m, has a surface expression that is about 1 m deep and 100 m wide today, and has distinct meander scrolls on the inside of the meander bend. The channel has been buried by a later, furrowed deposit to the south, and several fairly small channels may enter the main channel from the north. This is clearly a relict channel that must have been active when the channel was on dry land, perhaps from 15,500 to 12,400 years ago (Lewis and Stone, 1991; Uchupi et al., 1999; Lewis, 2014). While the timing of the arrival of the modern humans of North America is not well known, they are thought to be present as early as 15,000 years ago (Gobel et al., 2008). If modern humans were present in the area of Long

Island Sound prior to 12,400 years ago, then they may have had a presence near this river and indeed elsewhere in the Long Island Sound basin.

At least two anthropogenic features are present in Figure 28. A slightly squiggly, east-west trough in the northern part of the figure is possibly caused by a ship dragging something, possibly an anchor. The straight, diagonal line trending west-northwest trough near the north edge of the figure is a communications cable.

Anthropogenic features in the Phase IV Area

There are a variety of anthropogenic features in the area that will be illustrated and briefly described. Shellfish dredging is common in the area to recover transplanted shellfish from leased lands. The crisp, circular but truncated grooves in Figure 29, water depth 9 m, were created in the 3.5-day gap between when the southern part of the figure was surveyed and when the northern part was surveyed. While it is not known how quickly the shellfish dredge tracks degrade, tracks in different stages of decay are observed throughout this figure. The increased backscatter (Figure 29) near the fresh dredge track is likely caused by the increased surface roughness created by the dredge. Older tracks show only a slightly elevated backscatter.

The seabed appears to be much more disturbed in Figure 30, water depth 12 m, and some possible circular tracks can be identified, although the patchy distribution of scoured areas suggest some localized erosion. High backscatter also suggests a variable but generally coarse sediment texture over a wide area. Note the diagonal topographic and low backscatter feature going towards the north-northeast, which is the path of the Iroquois gas pipeline. NOAA hydrographic survey H11044 mapped this area using side-scan sonar in 2001 (McMullen et al., 2005), and the seabed character was possibly quite different at that time than it was at the time of our Phase IV survey (Figure 31). In particular, Poppe et al. (2008) noted a pattern of downslope-trending, low backscatter features which could be connected to form a channel network (left-hand side of Figure 31) and their cores in the area shows some buried shelly sand layers while the backscatter image from our Phase IV multibeam survey (right-hand side of Figure 31) shows a diffuse high-backscatter pattern. A likely explanation for the backscatter change between the two surveys is that the bottom was reworked by one or more high shear stress event between the 2001 and 2022, and coarser material that was buried in 2001 is at the surface in 2022. A part of the overlap area was also imaged during the 2014 LISPilot survey. That backscatter record differed from both the 2001 and the 2022 surveys and showed generally high backscatter lineations that trended northeast-southwest. Again, a likely explanation is that occasional high shear stress events are periodically reworking the seafloor in this area, which reinforces the idea that there can be significant temporal variability in sedimentary processes, especially in shallower water. It is possible that the downslope-trending, low backscatter strips mentioned by Poppe et al. (2008) are related to the sinuous troughs described for other regions of the Phase IV

study area. Those topographic features, which form through the dewatering and compaction of thick glacial and post-glacial lake sediments, could create topography that collects fine-grained sediments during periods of weak currents and low bed shear stress.

Figure 32, water depth 16 m, appears to provide an example of spatial variability in sedimentation patterns. The top half of the image shows a pockmarked seabed while the central portion of the image shows a seabed that is much smoother. The patches of higher backscatter in the bottoms of the pockmarks are consistent with observations in other areas while the area with the smoothed seafloor has a distinctly lower backscatter with maybe no patches of higher backscatter. The seabed in the bottom quarter of the image is a bit more irregular than the central portion but less irregular than the northern half of the image, yet there are few areas of higher backscatter. There is a slight but distinct topographic step of less than 0.05 m between the region with the pockmarked seabed in the north and the region with the smoothed seafloor in the center of the image. The step, which is less pronounced towards the west, can be depositional or erosional in origin with either enhanced deposition in the central zone, enhanced erosion in the northern half, or a combination of both processes.

Several other anomalous, anthropogenic features were also observed that should be mentioned. Figures 33 and 34, water depths 12 m and 16 m, show somewhat rectangular features that were likely created by dropping materials from a ship that was following a rectangular pattern. The area of the deposit in Figure 33 is about 500 m on a side and composed of thinner features that are about 10 m to 20 m wide and with a maximum relief of less than 0.05 m to 0.2 m, but the features are not resolved on the backscatter image suggesting that they are buried. The overall deposit in Figure 34 is about 600 m by 1,100 m and is composed of thinner features that are also about 0.05 m to 0.2 m high and about 10 m to 20 m wide, but here the features are resolved on the backscatter image perhaps suggesting that the deposit is more recent. This deposit was also imaged by the H11044 side-scan sonar survey done in 2001. One more feature of similar dimensions was imaged at 41º 10.141'N 73º 00.909'W, water depth 14 m, but that feature is only identified based on the backscatter data. There is no topographic expression.

Marks made by shellfish dredging and by dragging anchors or possibly other gear on the seabed can be seen in many parts of the Phase IV survey. However, somewhat different drag marks appear in several areas (Figure 35, water depth 24 m; see also similar drag marks on Figure 32). The drag marks appear to be bundles of individual features that extend for long distances as mostly straight lines, and on Figure 35 two sets of drag marks intersect. The individual grooves have depths of about 0.1 m and widths of maybe 2 m, and they are difficult to measure when the grid size is 1 m. They are found in low backscatter, muddy sediments they do not continue in high backscatter, coarser, sediments. One possible origin for these bundles of drag marks is that vessels, possibly barges being pulled or pushed by tugs, are dragging cables (i.e., wire ropes) along the seafloor as they move between ports. Multibeam survey data

collected during Phase III A (collected by SoMAS in 2023) substantiates this interpretation because similar seabed features are observed to originate or terminate at the Northport Terminal that lies about 1.5 miles offshore of the Northport Power Station. The Northport Terminal has been a frequent stop for barges delivering oil to the Northport Power Station and the drag marks are likely to be associated with that barge movement.

Since the barges and tugs move between the same sets of local ports, the drag marks end up in the same place on the seafloor. The locations of the bundles of drag marks were compared with compilations of vessel traffic areas available on the Connecticut Blue Plan website (https://maps.cteco.uconn.edu/projects/blueplan/layersshua/#traffic) and at Marine Vessel Traffic (https://www.marinevesseltraffic.com/LONG%20ISLAND%20SOUND/ship-traffic-tracker#gotomap), but there was no alignment between the more popular vessel tracks and the drag marks, suggesting that not all vessels in LIS are dragging cables.

One of the more remarkable objects we found during our survey was an oblong feature that is labeled as a rock on NOAA chart 12354 (Figure 36, water depth 14 m), but this feature or deposit doesn't look like a typical rock outcrop or a debris pile when looking at the gridded data. Some additional analysis of this feature seems appropriate to better understand its origin. The images in Figure 36 are based on depth and backscatter gridded at 1 meter, so a new grid was created with a 0.25 m gridding interval (Figure 37). The feature has approximate heights of 0.5 m and widths of 30 m at its west end, 0.3 m and 60 m at its east end, and 0.2 m and 30 m at its midpoint. The west end of the deposit is well defined while the east end of the deposit is more diffuse, and the length of the feature is about 350 m. The surface of the west end of the feature appears smooth while the east end has a different character with many larger blocks with apparent horizontal dimensions of about 5 m and some with heights up to 1.5 m. The different characters of the west end and the east end of the feature lead to the suggestion that this feature may be made up of two deposits, an initial deposit of at the west end and a later deposit at the east end. The axes of the two deposits appear to be offset by 15 m to 20 m with the axis of the eastern deposit offset to the south of the western deposit. This is also consistent with there being two anthropogenic deposits.

Conclusions

This project collected high-resolution multibeam bathymetric and backscatter data from the Phase IV study area of the LIS Seafloor Habitat Mapping Initiative. The data products generated by the project will help provide a foundation for interpreting sedimentological, biological, oceanographic, and other data collected by the project. The bathymetric data

collected during the three project cruises agree well internally, and the depths determined also agree well with adjacent hydrographic surveys done previously by NOAA for charting purposes. Many natural features of interest are described that may be of importance in understanding the benthic habitat of the study area, and the anthropogenic features observed will help to understand our impacts on this environment. Comparison with prior surveys done in the area show that sedimentary processes are modifying the seafloor, perhaps due to high bed shear stresses created during storm conditions when there are strong currents and large waves. It is expected that our interpretations will evolve and improve as new data is collected in the Phase IV area by other investigators, and it is anticipated that some of the observations made in this report will help guide future observations and interpretations.

Acknowledgments

A number of individuals have participated in this project and are quite responsible for the success of the project. Dr Mohamed Elsaied, Senior Postdoctoral Scientist at SoMAS, and Jason Mueller, Graduate Student at SoMAS, participated in the shipboard data collection efforts on the R/V *Connecticut* and the R/V *Seawolf* as well as in setting up and removing the equipment from the ships. Wendy Woods and Dennis Arbige from UConn also joined our shipboard scientific party and made valuable contributions. The captains and crews of the R/V *Connecticut* and R/V *Seawolf* contributed their expertise to ensure the success of the project and kept us on track! Dr Elsaied assisted materially in the processing of the voluminous multibeam data and he was especially important working with software vendors to make successful data processing possible. This project has been funded wholly or in part by the United States Environmental Protection Agency under assistance agreement LI-00A00579-0 to the Connecticut Department of Energy and Environmental Protection (DEEP). The contents of this document do not necessarily reflect the views and policies of DEEP or the State of Connecticut or of the Environmental Protection Agency, nor does DEEP or the EPA endorse trade names or recommend the use of trade names or recommend the use of commercial products mentioned in this document.

References Cited

Battista, T, Sautter, W, Kagesten, G, (2017). Bathymetry and acoustic backscatter collected in Long Island Sound for the Phase I Long Island Sound Seafloor Mapping Project 2014 (NCEI Accession 0167946). NOAA National Centers for Environmental Information. Dataset. https://www.ncei.noaa.gov/archive/accession/0167946.

Buczkowski, B.J., Reid, J.A., Schweitzer, P.N., Cross, V.A., and Jenkins, C.J., 2020, usSEABED—Offshore surficial-sediment database for samples collected within the United

States Exclusive Economic Zone: U.S. Geological Survey data release, https://doi.org/10.5066/P9H3LGWM. Also accessed at https://www.usgs.gov/programs/cmhrp/science/accessing-usseabed.

Bokuniewicz HJ, Gordon RB, 1980. Sediment transport and deposition in Long Island Sound. Adv Geophys 22:69–106.

Cartwright, JA, Lonergan, L, 1996, Volumetric contraction during the compaction of mudrocks: a mechanism for the development of regional-scale polygonal fault systems: Basin Research, v. 8, no. 2, p. 183–193.

Cartwright, JA, Wattrus, NJ, Rausch, DE, Bolton, A, 2004, Recognition of an early Holocene polygonal fault system in Lake Superior: Implications for the compaction of fine-grained sediments: Geology, v. 32, no. 3, p. 253–256.

Cerrato, R.M., A.M. Flanagan, R.D. Flood. 2015. Haverstraw Bay Benthic Habitat Characterization. Marine Sciences Research Center Special Report No. 141, Stony Brook University, Stony Brook, NY, 57 pp downloaded from https://commons.library.stonybrook.edu/somas_articles/2/

Durran, DR, (1986). Another look at downslope wind storms, Part I: On the development of analogs to supercritical flow in an infinitely deep, continuously stratified fluid. J .Atmos. Sci. 43, 2527-2543.

Fairbanks, RG, 1989. A 17,000-year glacio-eustatic sea level record: influence of glacial melting rates on the Younger Dryas event and deep-ocean circulation. Nature 342, 637-642.

Ferrini, VL, Flood, RD (2001). Sedimentary characteristics and acoustic detectability of ship-derived deposits in western Lake Ontario. J. Great Lakes Res. 27(2): 210-219.

Ferrini VL, Flood RD (2006) The effects of fine-scale surface roughness and grain size on 300 kHz multibeam backscatter intensity in sandy marine sedimentary environments. Mar Geol 228:153–17

Flanagan, AM, Flood, RD, Maher, NP, Cerrato, RM (2019) Quantitatively characterizing benthic community-habitat relationships in soft-sediment, nearshore environments to yield useful results for management. J. Environmental Management 249:109361. https://doi.org/10.1016/j.jenvman.2019.109361

Flood, RD (1983). Classification of sedimentary furrows and a model for furrow initiation and evolution. Geological Society of America Bulletin, 94, 630-639.

Flood, RD (1988). A lee wave model for deep-sea mudwave activity. Deep Sea Research Part A. Oceanographic Research Papers 35(6): 973-983.

Flood, RD, Johnson, T C, 1984. Side-scan sonar targets in Lake Superior-evidence for bedforms and sediment transport. Sedimentology 31:311-333.

Fonseca L, Mayer L (2007) Remote estimation of surficial seafloor properties through the application Angular Range Analysis to multibeam sonar data. Mar Geophys Res 28:119–126

Goebel, T, Waters, MR, O'Rourke, D.H., 2008. The Late Pleistocene Dispersal of Modern Humans in the Americas. Science 319: March 14, 1497-1502.

Hughes Clarke JE (1994) Toward remote seafloor classification using the angular response of acoustic backscattering: a case study from multiple overlapping GLORIA data. IEEE J Ocean Eng 19(1):112–126

Hughes Clarke JEH, Mayer LA, Wells DE (1996) Shallow-water imaging multibeam sonars: A new tool for investigating seafloor processes in the coastal zone and on the continental shelf. Mar Geophys Res 18:607-629

Knebel HJ, Poppe LJ (2000) Sea-Floor Environments within Long Island Sound: A Regional Overview. Journal of Coastal Research 16(3):533-550.

Latimer, JS, Tedesco, MA, Swanson, RL, Yarish, C, Stacey, PE, Garza, G (2014) Long Island Sound. Springer Series on Environmental Management, Springer New York Heidelberg Dordrecht London. DOI 10.1007/978-1-4614-6126-5 ISBNs 978-1-4614-6125-8, 978-1-4614-6126-5

Lewis, R (2014) The Geology of Long Island Sound. In: Latimer, JS, Tedesco, MA, Swanson, RL, Yarish, C, Stacey, PE, Garza, G (Eds)(2014) Long Island Sound. Springer Series on Environmental Management, Springer New York Heidelberg Dordrecht London. 47-77.

Lewis, RS, Digiacomo-Cohen, M, 2000. A Review of the Geologic Framework of the Long Island Sound Basin, With Some Observations Relating to Postglacial Sedimentation. Journal of Coastal Research, 16(3), 522-532.

Lewis, RS, Stone, JR. 1991, Late Quaternary stratigraphy and depositional history of the Long Island Sound Basin: Connecticut and New York: Journal of Coastal Research, Special Issue 11, Fall 1991, p. 1–23.

Lurton, X.; Lamarche, G. (Eds) (2015) Backscatter measurements by seafloor-mapping sonars. Guidelines and Recommendations. 200p. http://geohab.org/wp-content/uploads/2014/05/BSWGREPORT-MAY2015.pdf

Lurton, X, Eleftherakis, D, Augustin, J-M (2018) Analysis of seafloor backscatter strength dependence on the survey azimuth using multibeam echosounder data. Mar Geophys Res 39:183–203

Mayer, LA (2006) Frontiers in seafloor mapping and visualization. Mar Geophys Res 27:7-17

McMullen KY, Poppe LJ, Paskevich VF, Doran EF, Moser MS, Christman EB, Beaver AL (2005) Surficial geology of the seafloor in west-central Long Island Sound as shown by sidescan sonar imagery. US Geological Survey Open-File Rep 2005-1018.

McMullen KY, Poppe LJ, Schattgen PT, Doran EF (2008) Enhanced Sidescan-Sonar Imagery, North-Central Long Island Sound: U.S. Geological Survey Open-File Report 2008-1174. Also available online at http://pubs.usgs.gov/of/2008/1174/

O'Donnell, J, Wilson, RE, Lwiza, K, Whitney, M, Bohlen, WF, Codiga, D, Fribance, DB, Fake, T, Bowman, M, Varekamp, J (2014) The Physical Oceanography of Long Island Sound. In: Latimer, JS, Tedesco, MA, Swanson, RL, Yarish, C, Stacey, PE, Garza, G (Eds)(2014) Long Island Sound. Springer Series on Environmental Management, Springer New York Heidelberg Dordrecht London. 79-158.

Office of Coast Survey (2022). Hydrographic Survey Specifications and Deliverables, NOAA Office of Coast Survey, Hydrographic Surveys Division, 187 pp. https://nauticalcharts.noaa.gov/publications/docs/standards-and-requirements/specs/HSSD_2022.pdf; Available at https://nauticalcharts.noaa.gov/publications/standards-and-requirements.html

Office of Coast Survey (2025). Hydrographic Survey Specifications and Deliverables, NOAA Office of Coast Survey, Hydrographic Surveys Division, 89 pp. https://nauticalcharts.noaa.gov/publications/documents/HSSD_2025-0-00.pdf; Available at https://nauticalcharts.noaa.gov/publications/standards-and-requirements.html

Peltier, WR, 1998. Postglacial variations in the level of the sea: Implications for climate dynamics and solid-Earth geophysics. Reviews of Geophysics 36: 441-689

Poppe, LJ; Knebel, HJ; Lewis, RS, Digiacomo-Cohen, ML 2002. Processes controlling the remobilization of surficial sediment and formation of sedimentary furrows in north-central Long Island Sound. Journal of Coastal Research, 18(4), 741-750. West Palm Beach (Florida)

Poppe, LJ, McMullen, KY, Williams, SJ, Crocker, JM, Doran, EF, 2008. Estuarine sediment transport by gravity-driven movement of the nepheloid layer, Long Island Sound. Geo-Marine Letters 28: 245-254.

Poppe LJ, Paskevich VF, Moser MS, DiGiacomo-Cohen ML, Christman EB (2004) Sidescan sonar imagery and surficial geologic interpretation of the sea floor off Branford, Connecticut: U.S. Geological Survey Open-File Report 2004-1003, CD-ROM; also available online at: http://pubs.usgs.gov/of/2004/1003/

Sánchez, N, Zeppilli, D, Baldrighi, E, Vanreusel, A, Lahitsiresy, MG, Brandily, C, Pastor, L, Macheriotou, L, García-Gómez, G, Dupré, S, Olu, K 2021. A threefold perspective on the role of a pockmark in benthic faunal communities and biodiversity patterns. Deep Sea Research Part I: Oceanographic Research Papers, 167, p. 103425.

Signell, RP; List, JH, and Farris, AS, 2000. Physical processes affecting the sea-floor environments of Long Island Sound. Journal of Coastal Research, 16(3), 551-566. West Palm Beach (Florida)

Uchupi, E., Driscoll, N, Ballard, RD, Bolmera, ST, 1999. Drainage of late Wisconsin glacial lakes and the morphology and late quaternary stratigraphy of the New Jersey-southern New England continental shelf and slope. Marine Geology 172: 117-145.

Weber, T.; Lurton, X. (2015) Chapter 2 - Background and fundamentals. In: Lurton, X.; Lamarche, G. (Eds). Backscatter measurements by seafloor-mapping sonars - Guidelines and Recommendations. 25-51. http://geohab.org/wp-content/uploads/2014/05/BSWG-REPORT-MAY2015.pdf

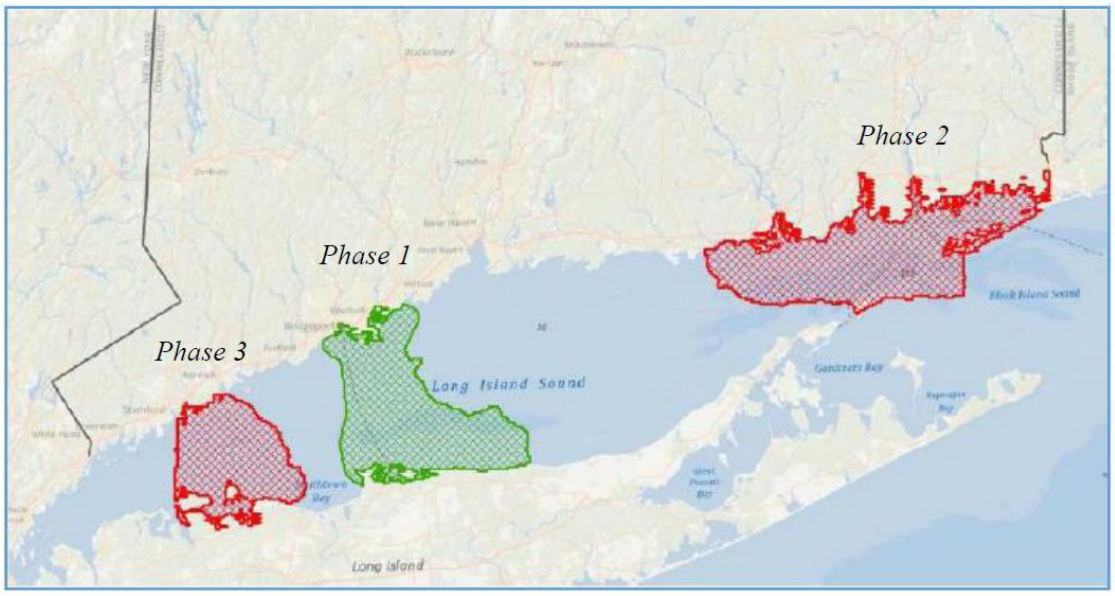

Figure 1. LIS Cable Fund Priority areas as of 2012.

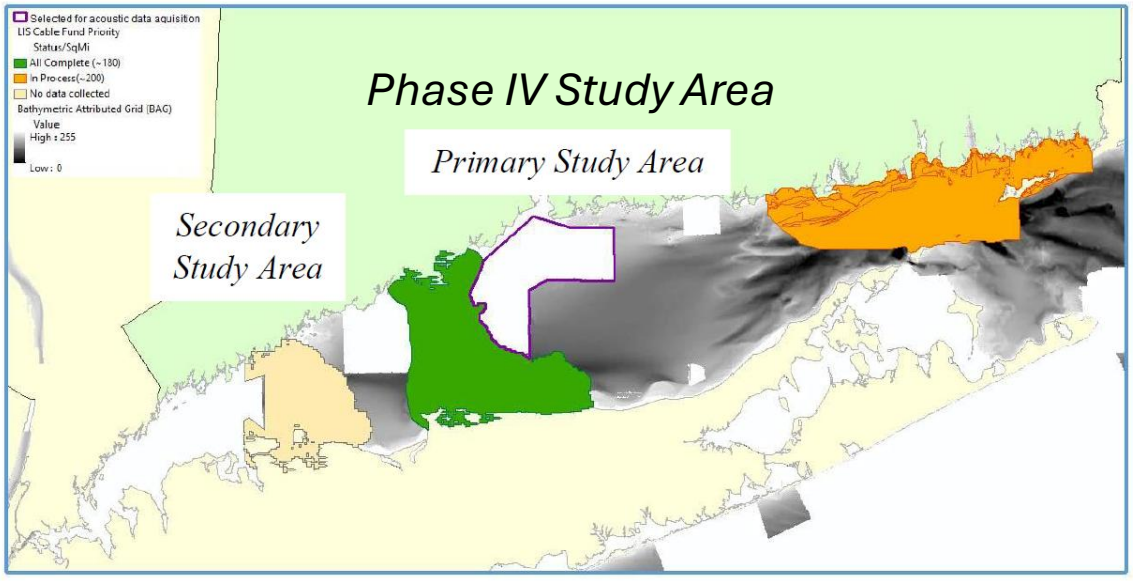

Figure 2. Map showing proposed area for acoustic data acquisition. The Primary Study Area is our Phase IV study area.

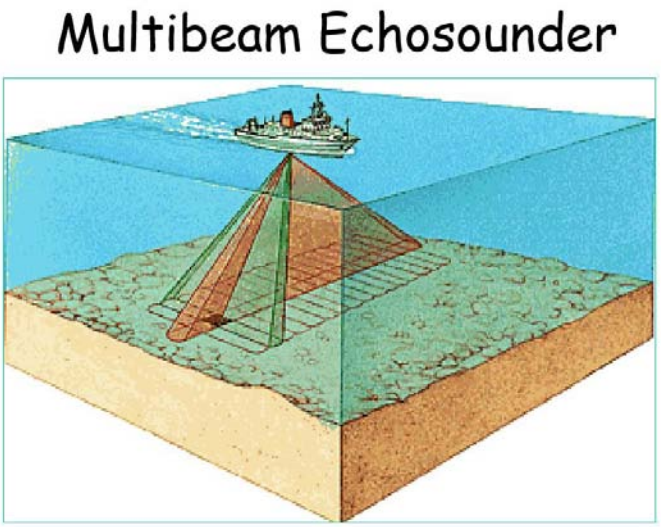

Figure 3. Graphic showing the operation of the multibeam echosounder (after Kongsberg). The transmit beam pattern is wide in the cross-track direction but narrow in the along-track direction while any one of the receiver beam patterns is narrow the cross-track direction but wide in the along-track direction. The water depth is determined where the transmit and receive beam patterns overlap.

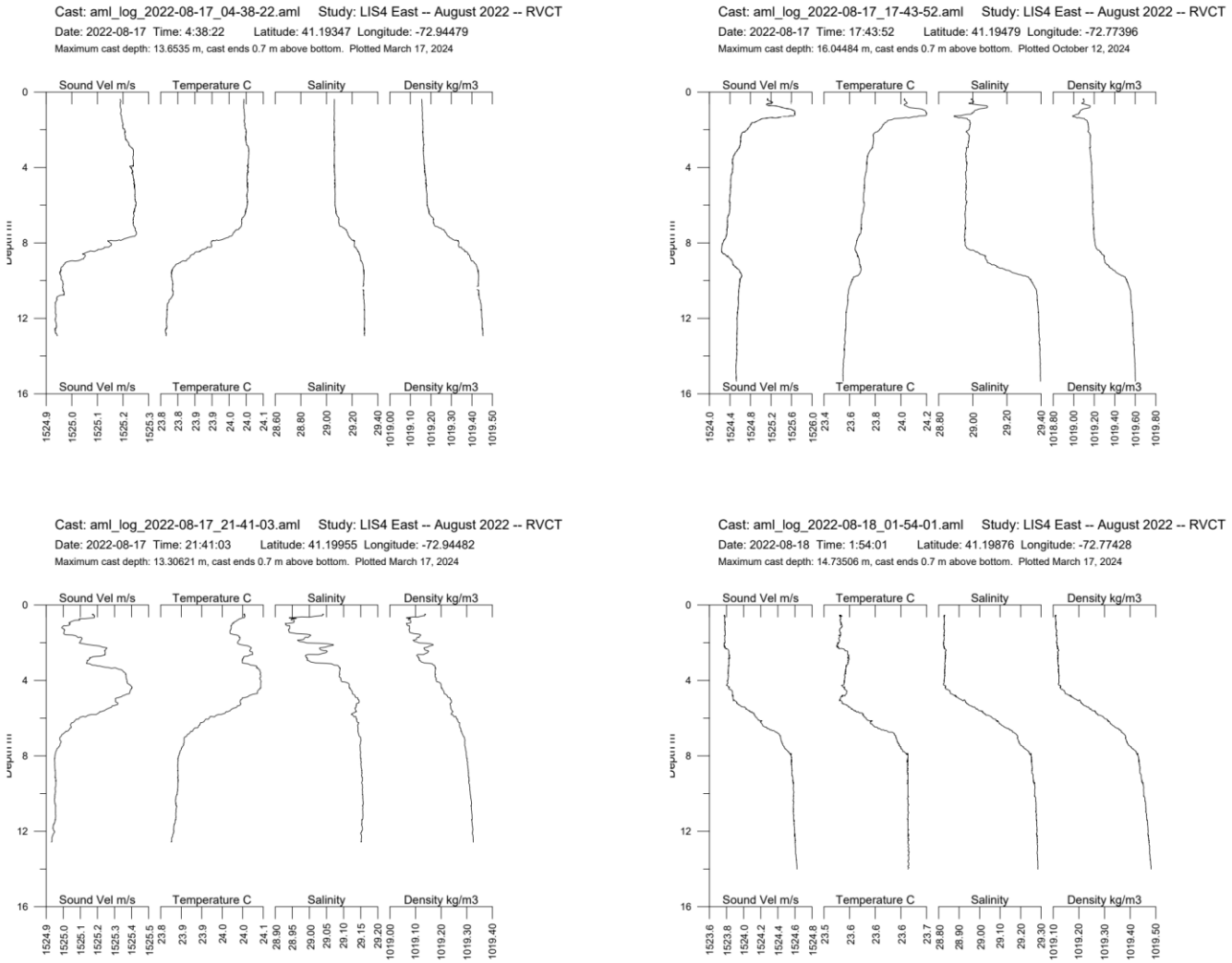

Figure 4. Four example sound velocity profiles collected during the survey in August, 2022. The sound velocity profile is needed to correct the sound pathways in the water column for refraction. Our profiler also reports temperature, salinity, and density which helps us understand what factors are controlling the velocity profile. Temperature and salinity are also needed to correct the backscatter record for attenuation in the water column.

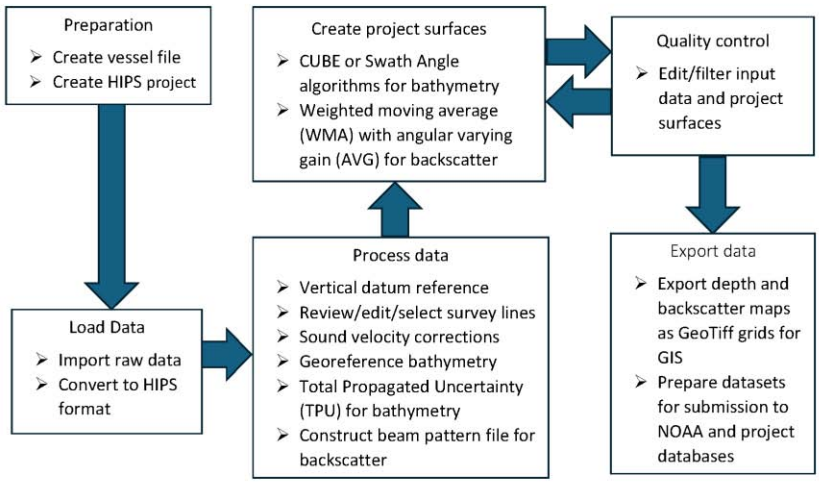

Figure 5. Workflow for multibeam data processing.

Figure 6. Multibeam system components used on the R/V *Connecticut*. Upper left: oblong Seapath GNSS satellite receiver mounted on lift arm. The yellow Trimble GNSS receiver is also visible. Right: lift arm with Seapath receiver positioned over top of moon pool (large tube with blue cover). Lower left: motion sensor (gray pressure case above plate) and multibeam transducer (red transducer below plate) in frame. The frame is bolted onto the bottom of the moon tube with diver assistance. The distances between the various devices need to be precisely known.

Figure 7. Multibeam system components used on the R/V *Seawolf*. Upper: oblong Seapath GNSS satellite receiver mounted on rail on winch deck. The yellow Trimble GNSS receiver and the yellow Fugro satellite receiver are also visible. Lower left: motion sensor (gray pressure case) and multibeam transducer (red transducer) mounted in frame. Lower right: The frame being lowered to the water. The frame is bolted onto the bottom of the moon tube with diver assistance. The distances between the various devices need to be precisely known.

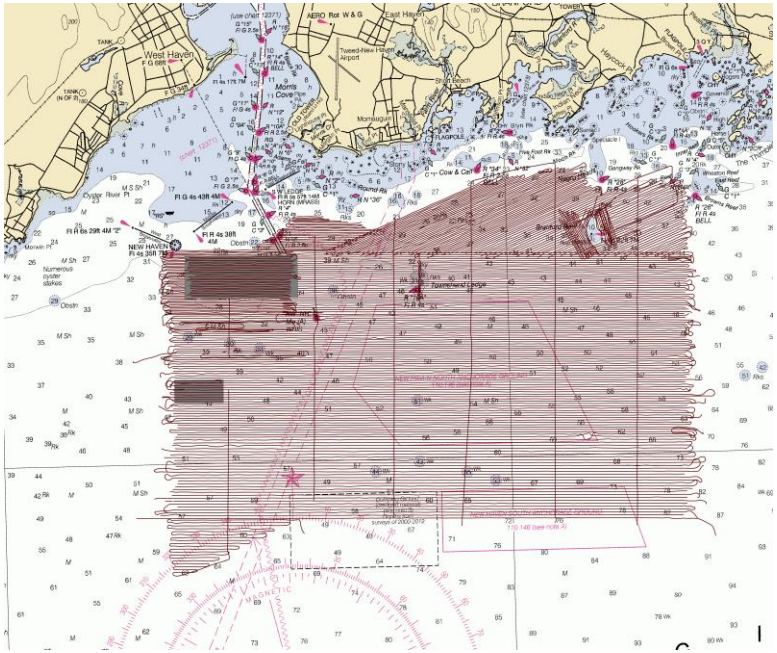

Figure 8. Ship tracks collected during the August, 2022 multibeam survey on the R/V *Connecticut*. The two gray boxes show the locations of the repeated survey areas. This survey is also named LIS4-East.

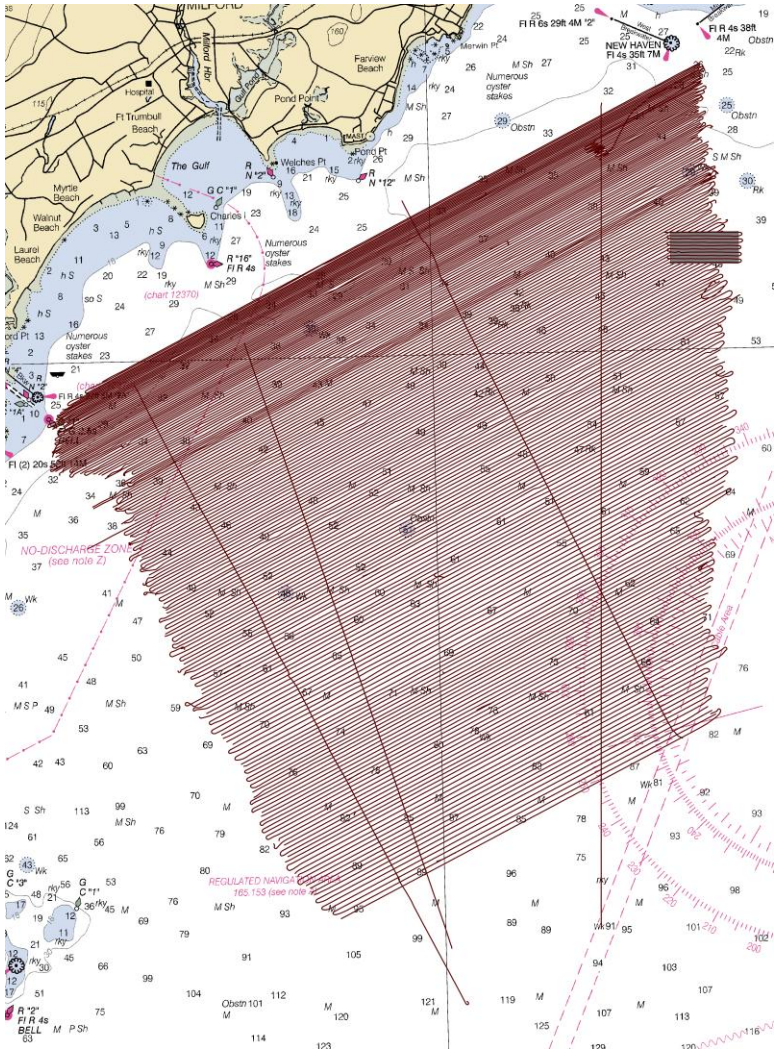

Figure 9. Ship tracks collected during the September, 2022 multibeam survey on the R/V *Seawolf*. The gray box shows the locations of the repeated survey area. This survey is also named LIS4-West-C.

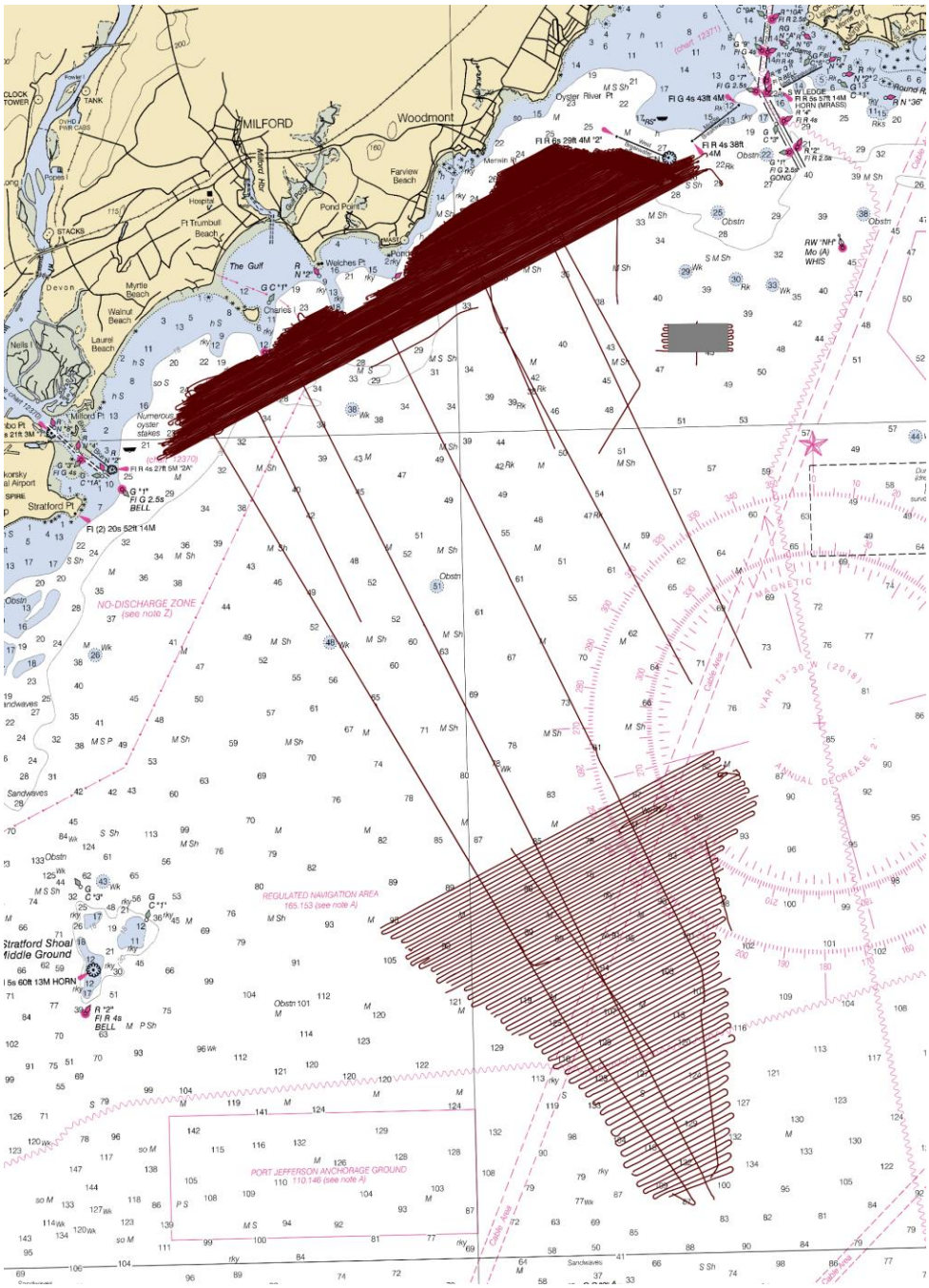

Figure 10. Ship tracks collected during the November-December, 2022 multibeam survey on the R/V *Seawolf*. The gray box shows the locations of the repeated survey area. The northern part of this survey is also named LIS4-West-N and the southern part of this survey is also named LIS4-West-S.

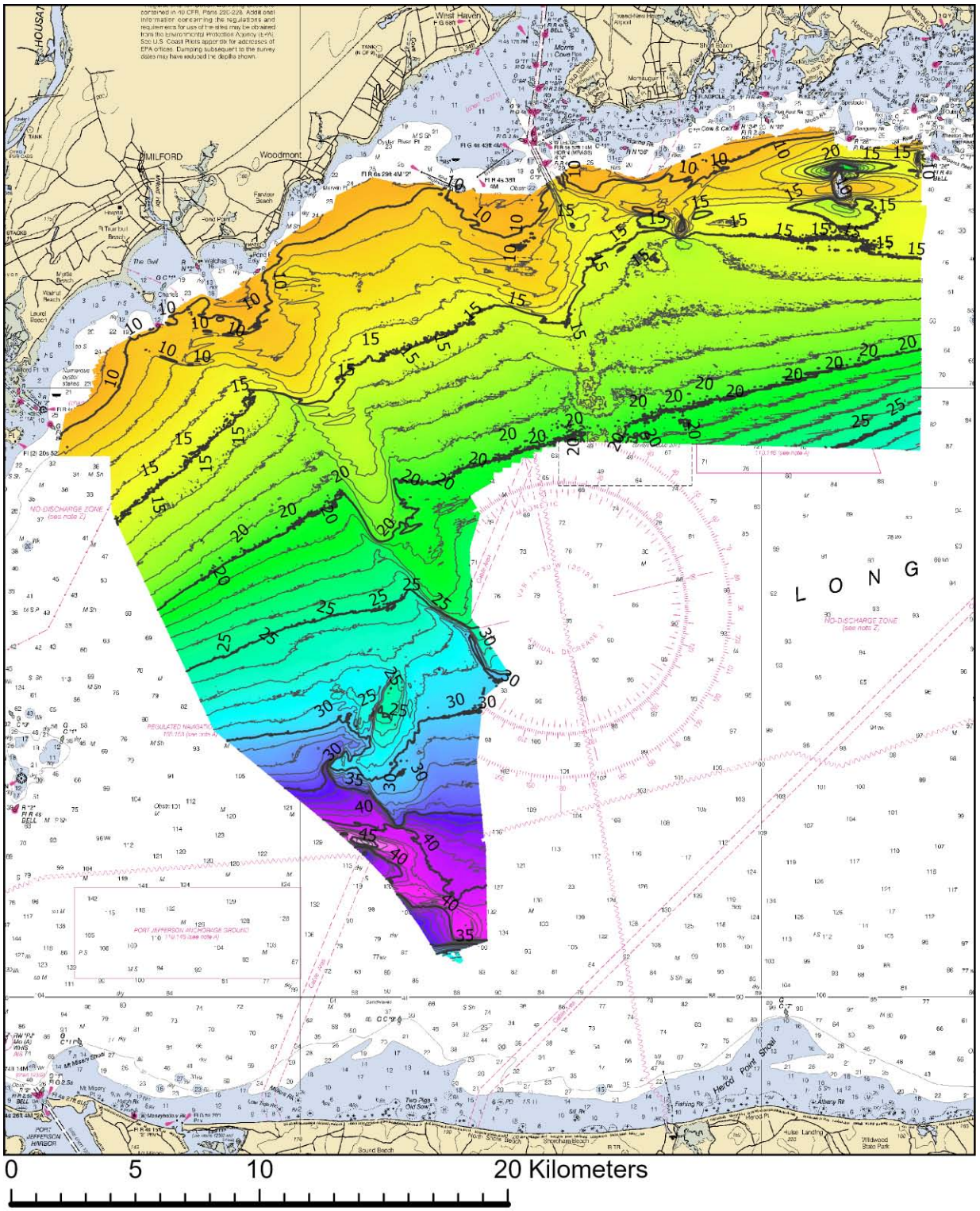

Figure 11. Bathymetry of the Phase IV study area. Contour interval 1 meter, vertical datum NAVD-88.

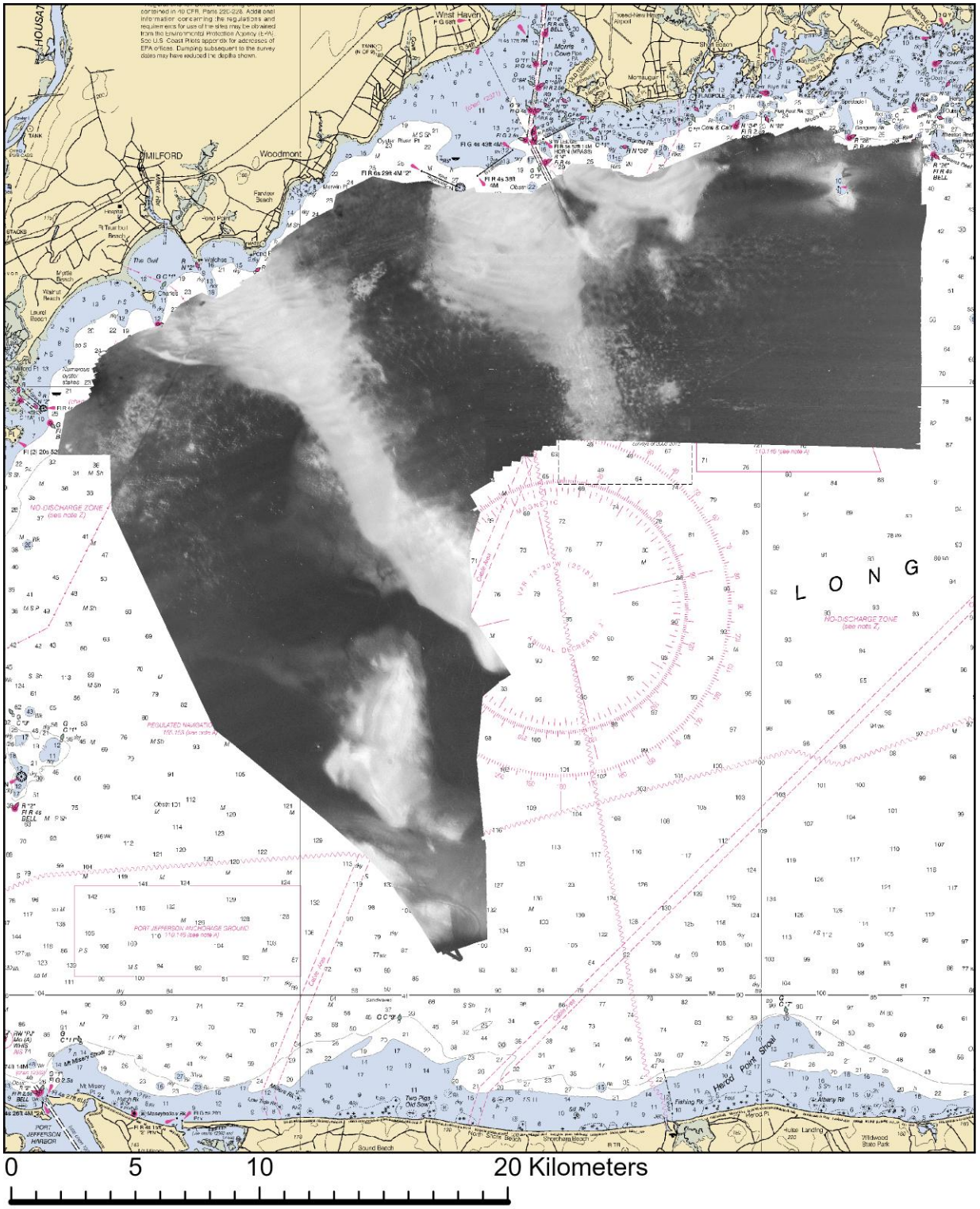

Figure 12. Acoustic backscatter of the Phase IV study area. Lighter color indicated a greater amount of backscatter.

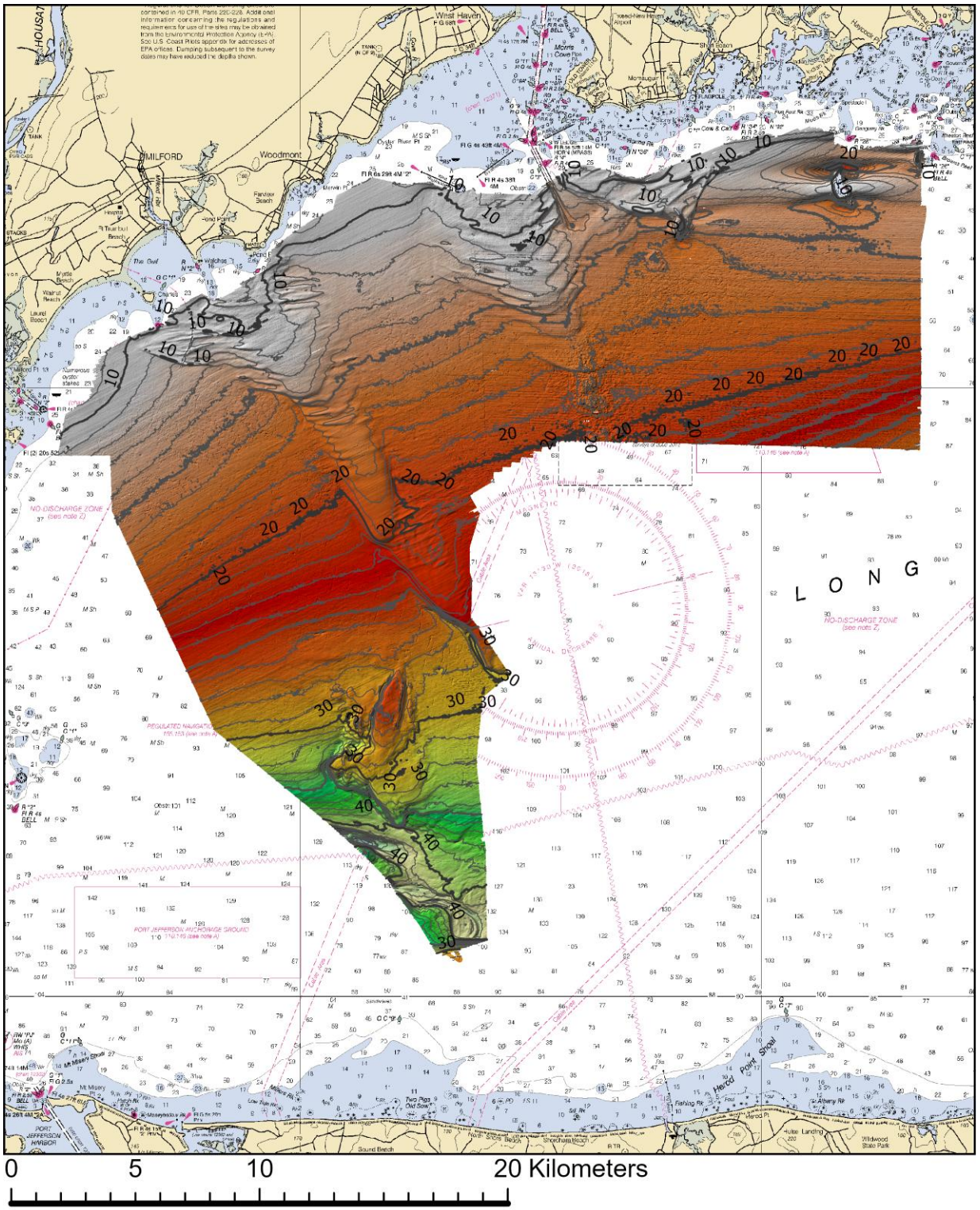

Figure 13. Bathymetry of the Phase IV study area displayed as hillshade image using ArcGIS Pro Shaded Relief symbology. Contour interval 1 meter, NAVD-88.

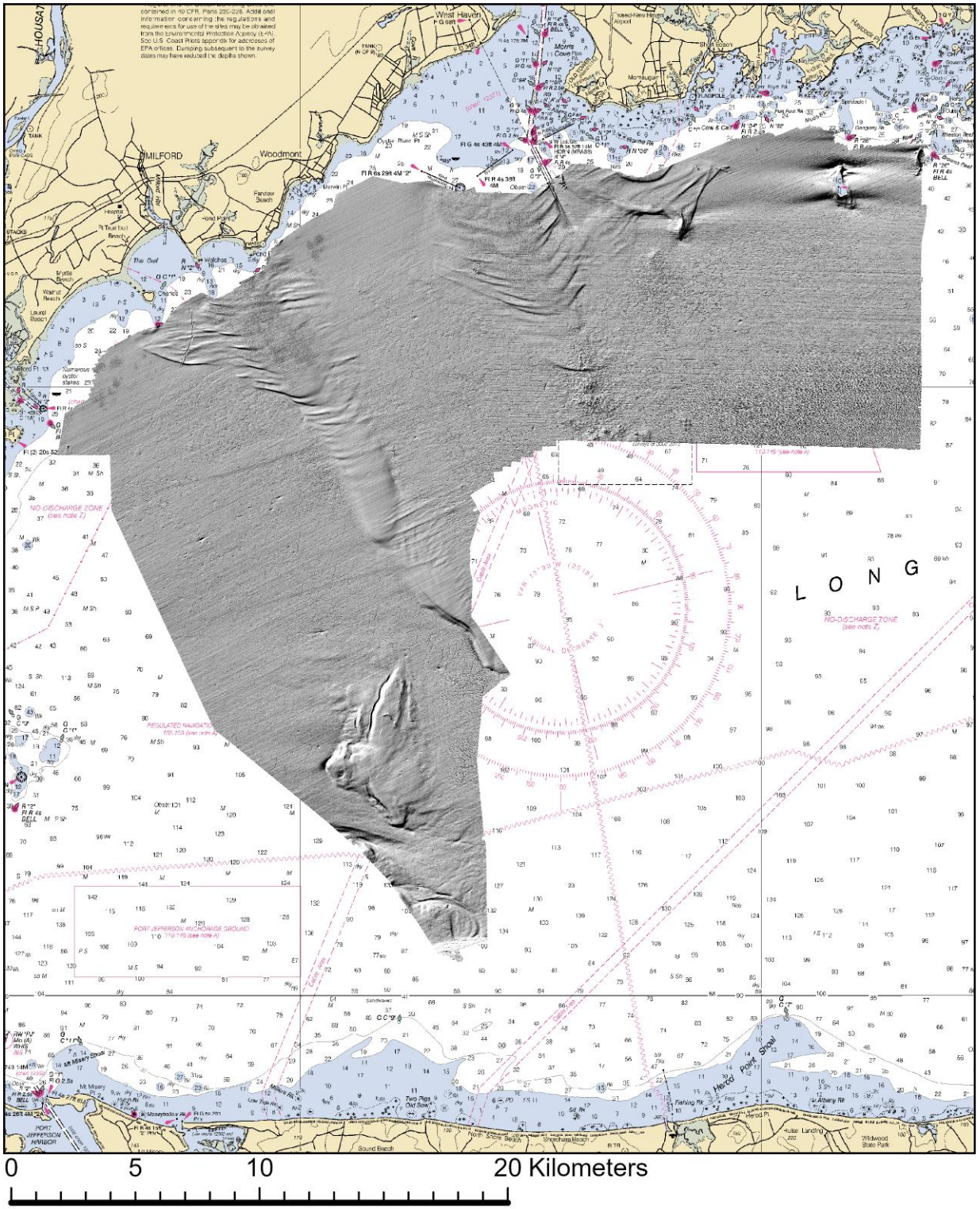

Figure 14. Hillshade image of the Phase IV study area bathymetry shaded with a synthetic sun in the northwest.

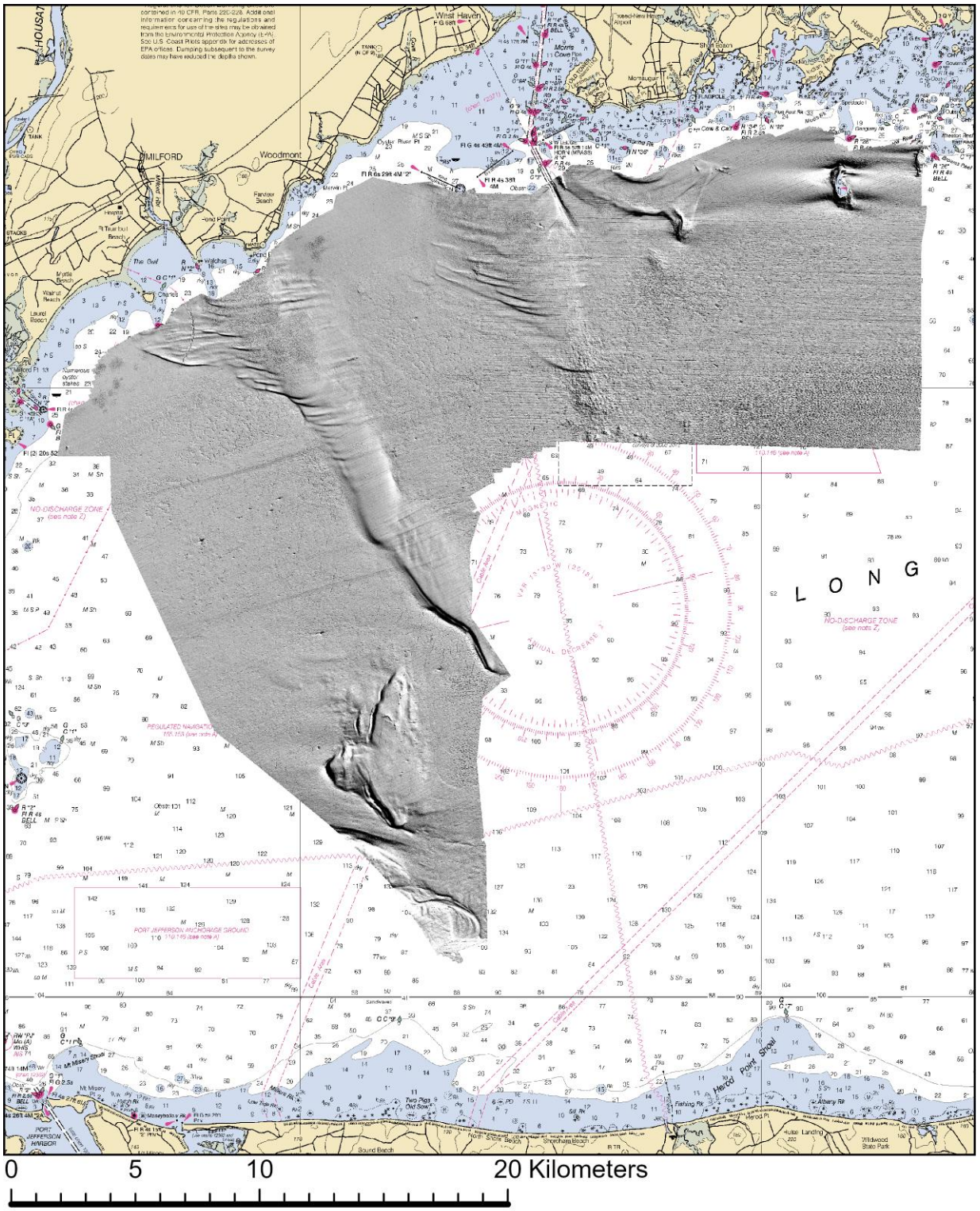

Figure 15. Hillshade image of the Phase IV study area bathymetry shaded with a synthetic sun in the northeast.

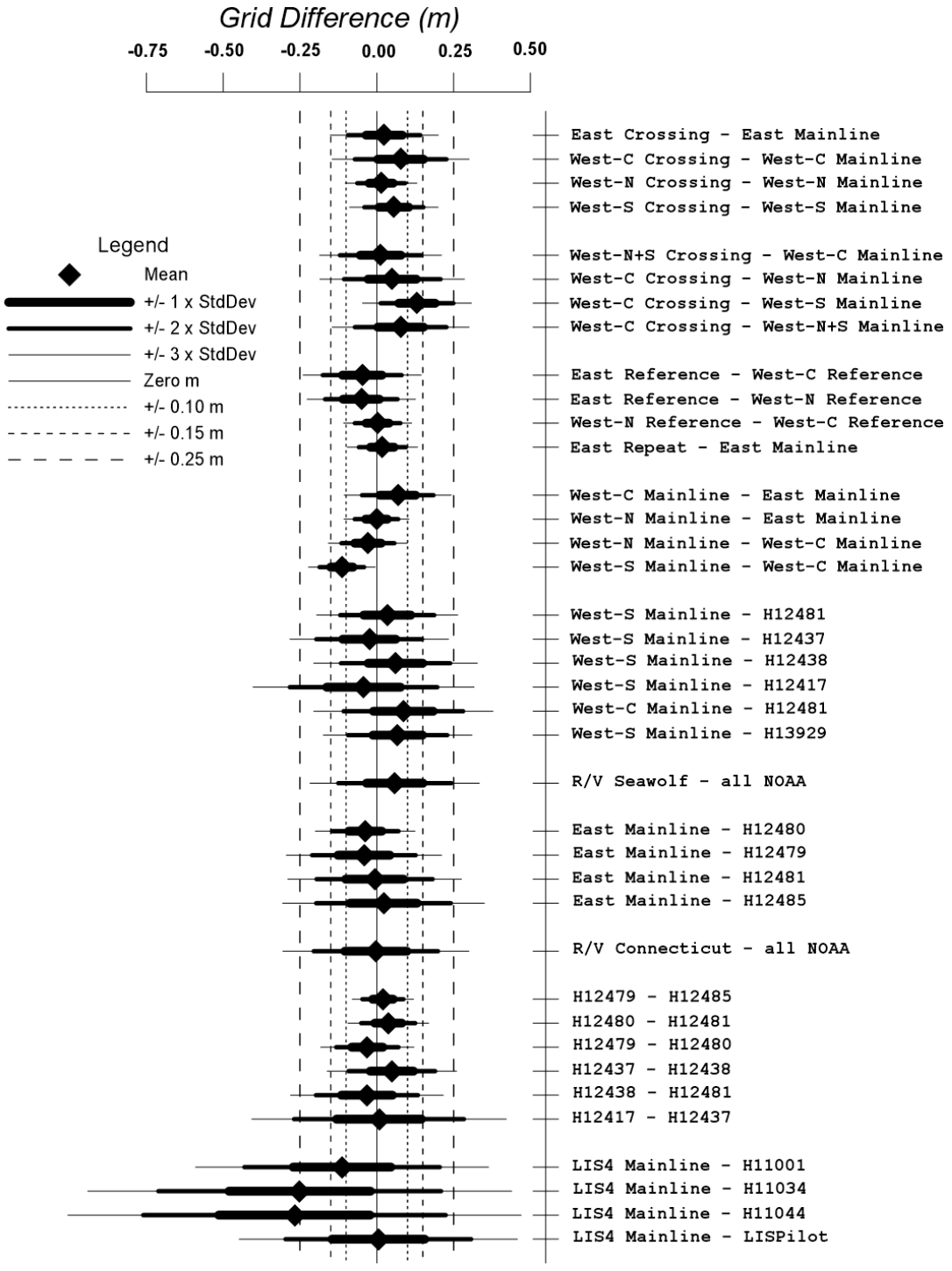

Figure 16. Compilation of grid comparisons between the various surveys of the Phase IV A (LIS4) multibeam mapping project and between the LIS4 surveys and adjacent NOAA hydrographic surveys. For a Gaussian distribution, 95% of the depth differences fall within two standard deviations of the mean. Surveys where 95% of the depth comparisons fall within +/- 0.25 m may meet the requirements for a "Critical" survey, but the depth difference comparison is only one component of the calculation of the vertical uncertainty.

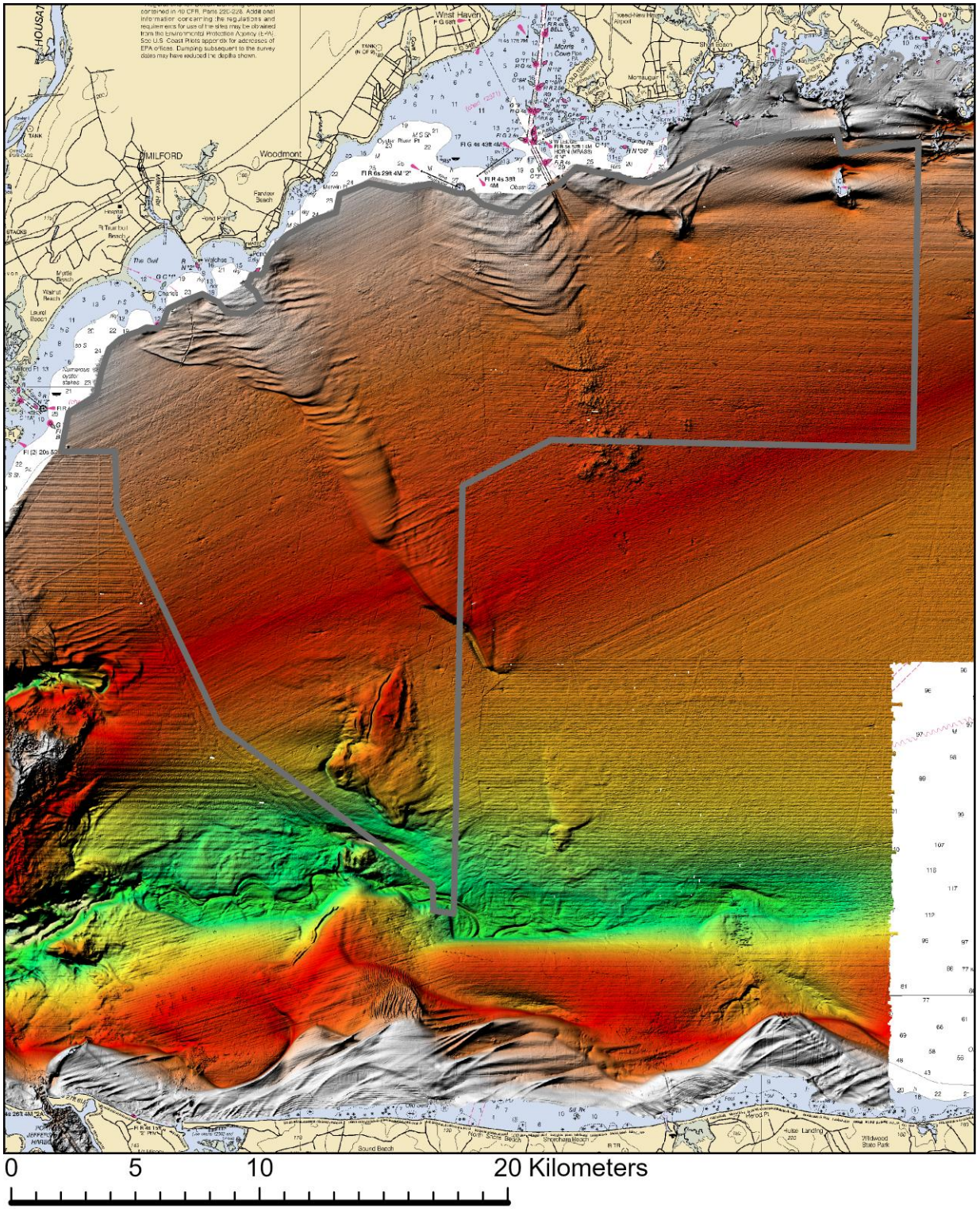

Figure 17. Compilation of bathymetric data from the Phase IV, LISPilot and NOAA hydrographic surveys. The bathymetry is displayed as hillshade image using ArcGIS Pro Shaded Relief symbology. Contour interval 1 meter, NAVD-88. Gray outline shows the limit of the Phase IV study area. Survey H13929 is not included in this figure.

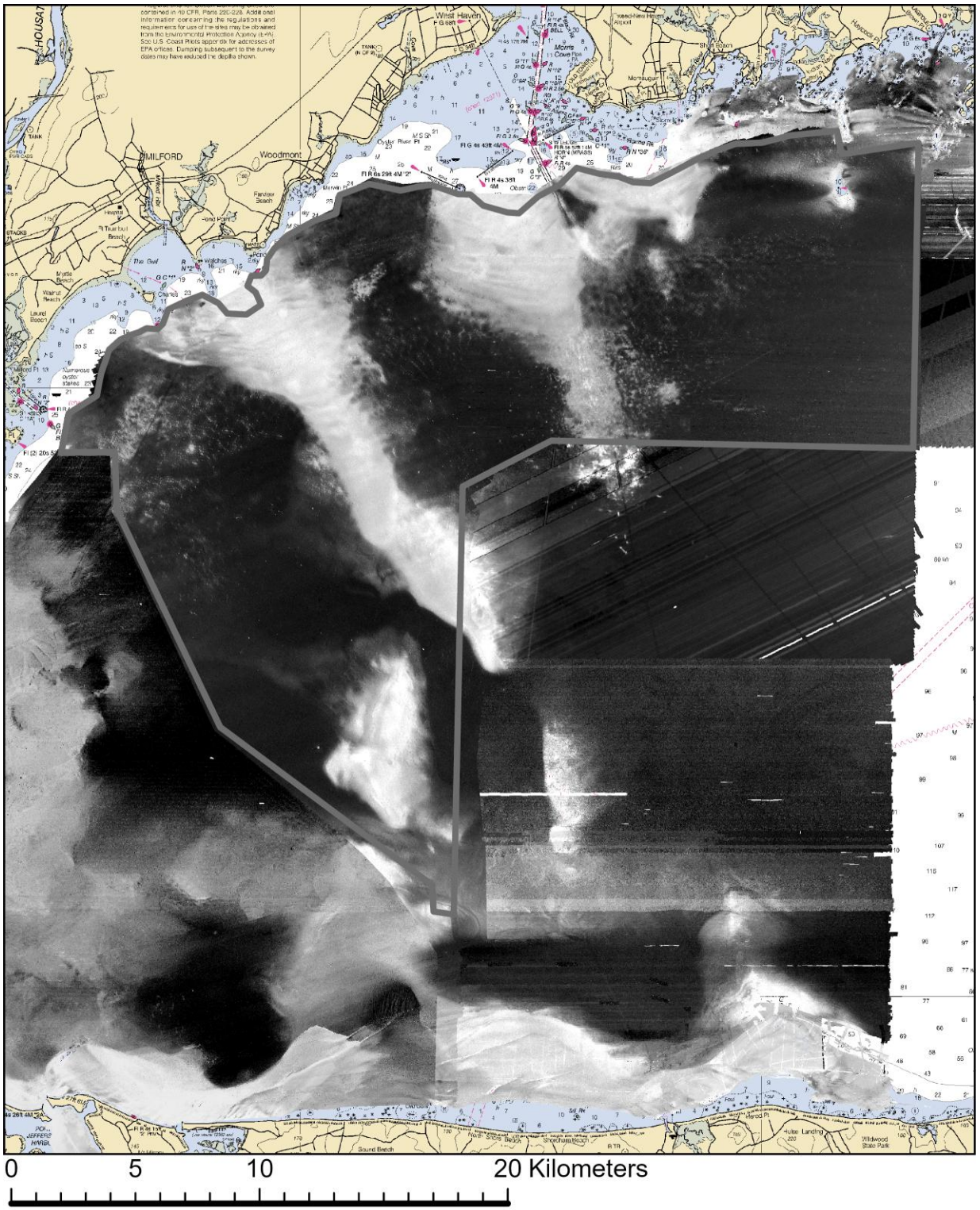

Figure 18. Compilation of backscatter data from the Phase IV, LISPilot and NOAA hydrographic surveys. Gray outline shows the limit of the Phase IV study area. Survey H13929 is not included in this figure.

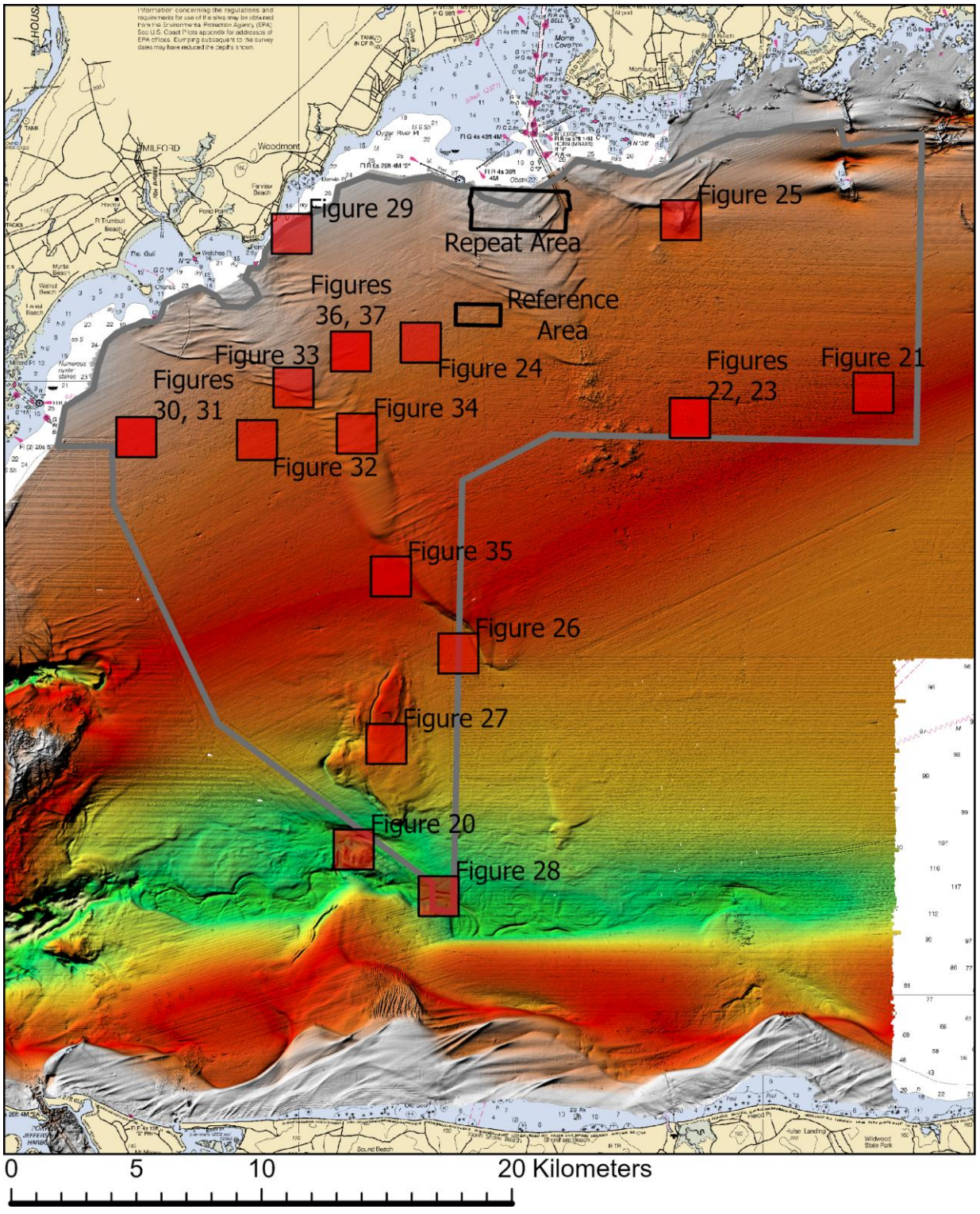

Figure 19. Index map showing the locations of Figures 20-37 (center point only), the Repeat Area and the Reference Area. Survey H13929 is not included in this figure.

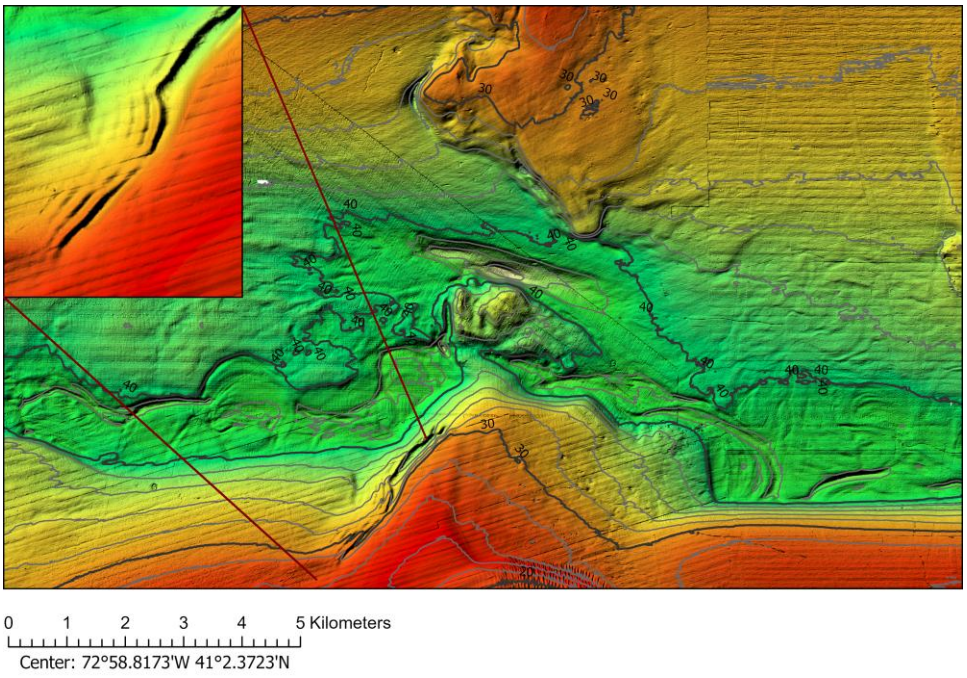

Figure 20. Shaded Relief map showing the meandering channel at the south end of the Phase IV study area. This channel probably was active from about 15,000 to 12,400 years ago when the post-glacial sea level was not high enough to allow sea water to enter Long Island Sound. The inset shows another example of a wavy seafloor on the west side of an escarpment in Long Island Sound. The periodic, wavy seafloor is probably related to internal waves generated as a stratified, west-ward flowing (flooding) tidal current flows over the topography. Contour interval 2 m. Figure locations are shown in Figure 19.

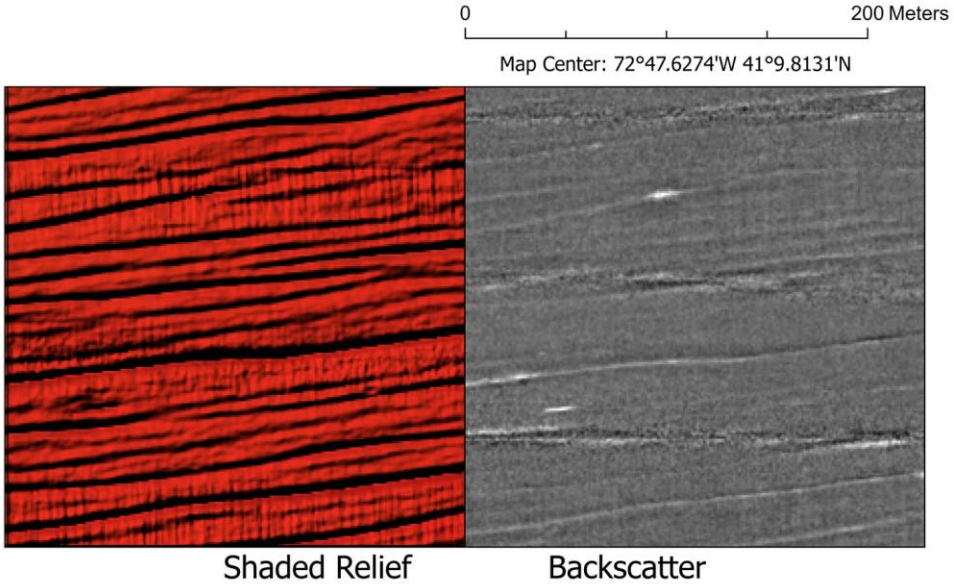

Figure 21. Example of furrowed topography in the Phase IV area, water depth 22 m. Left: shaded relief image of furrowed seabed topography. Furrows are likely due to periodically strong flood tidal flows moving from right to left. Right: multibeam backscatter mosaic of furrowed seabed topography. Comment applies to Figures 20 to 37: Colored dots indicate descriptions of sediment samples. Figure location shown in Figure 19.

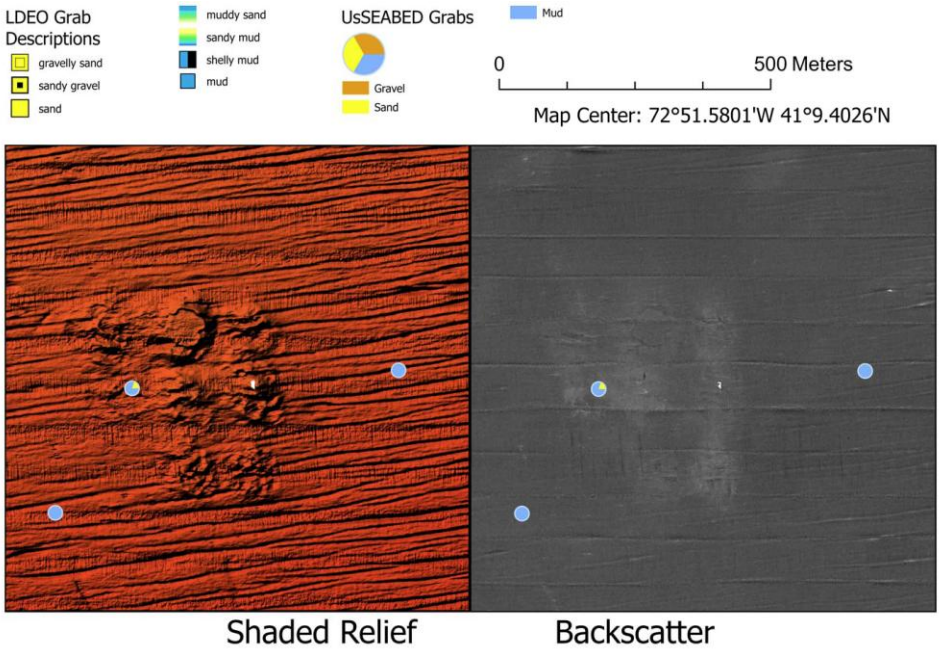

Figure 22. Dredge spoil mounds and furrows in the Phase IV area, water depth 20 m. Left: shaded relief image of dredge spoil mounds which often have cratered tops or, less commonly, flat tops. Furrows are also present in the area and some of the furrows appear to cut across the dredge spoil deposits. Right: multibeam backscatter mosaic showing dredge spoil deposits with higher reflectivity. This is an active disposal area for clean dredge spoils.

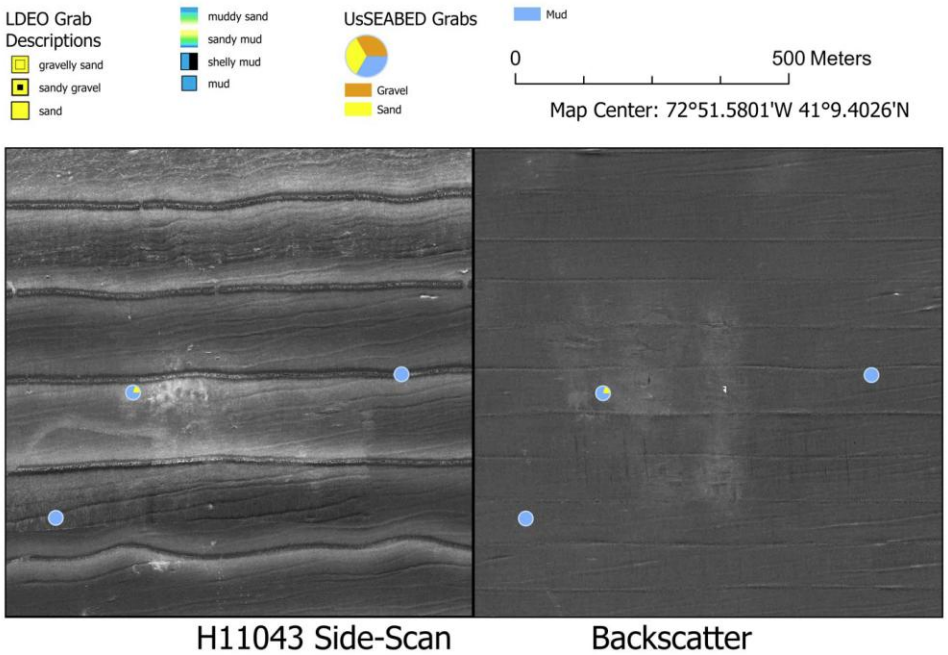

Figure 23. Left: side-scan sonar mosaic collected during H11043 showing the location of fewer dredge spoil deposits at that time. A furrowed seafloor is also visible. Right: multibeam backscatter mosaic collected in 2022 showing the existence of more dredge spoil deposits than were present in 2001.

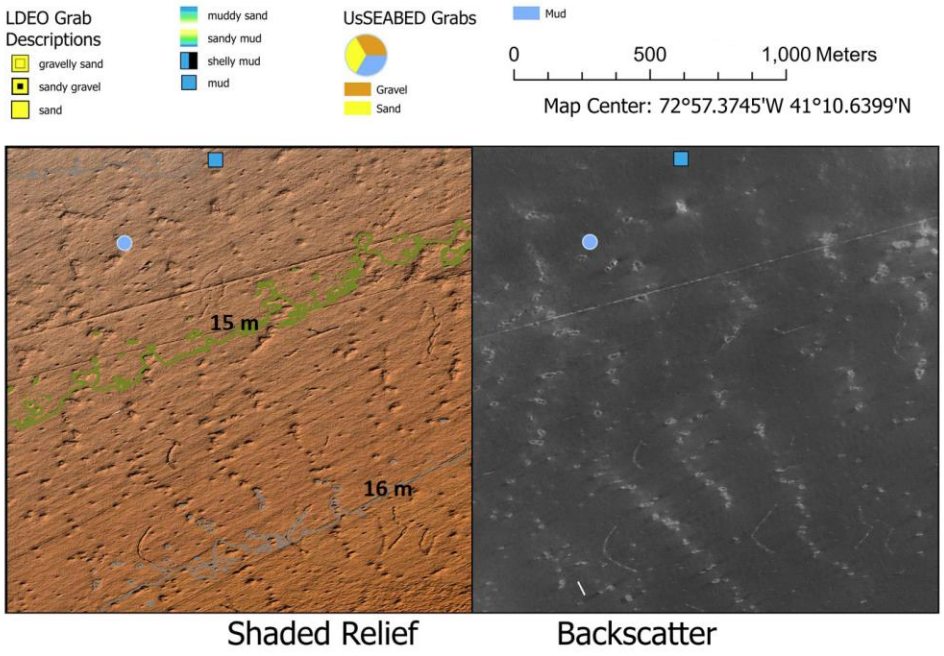

Figure 24. An area of lines of small pits, water depth 15 m. Left: shaded relief image of pits on the seafloor, apparently in lines. The pits have diameters of about 20 to 50 m and depths of 0.2 to 0.5 m. The linear feature in upper part of image was possibly created by an anchor being dragged. Left: multibeam backscatter mosaic showing that the floors of the small pits have higher backscatter, so the sediments there are likely coarser than the sediments in the surrounding areas.

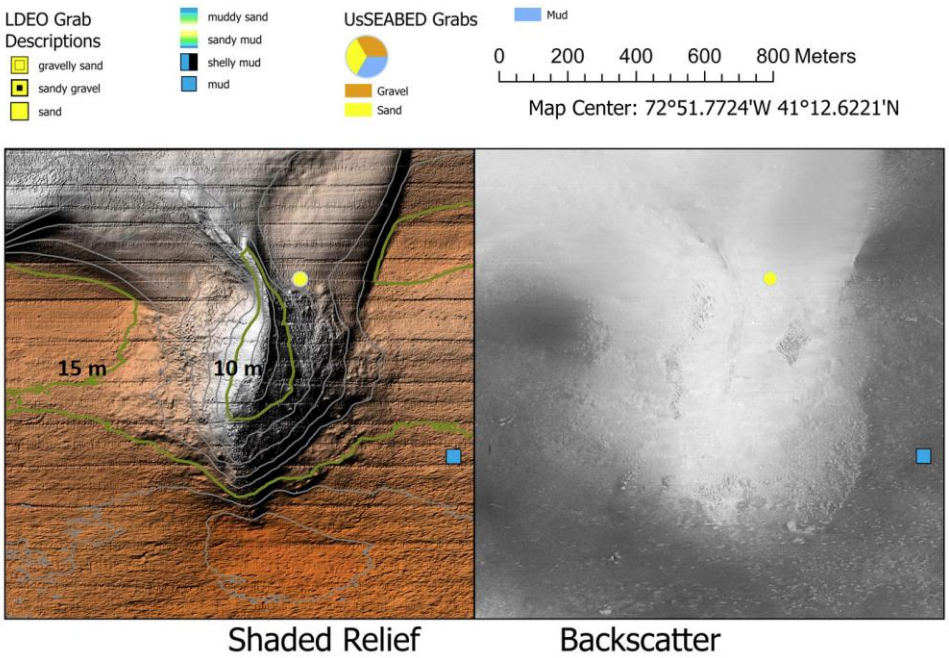

Figure 25. Townshend Ledge rises 7 m above the seafloor to a water depth of 8 m. Left: shaded relief image showing change in seafloor texture with distance from the ledge. Right: multibeam backscatter mosaic showing patterns of higher backscatter in the vicinity of the ledge.

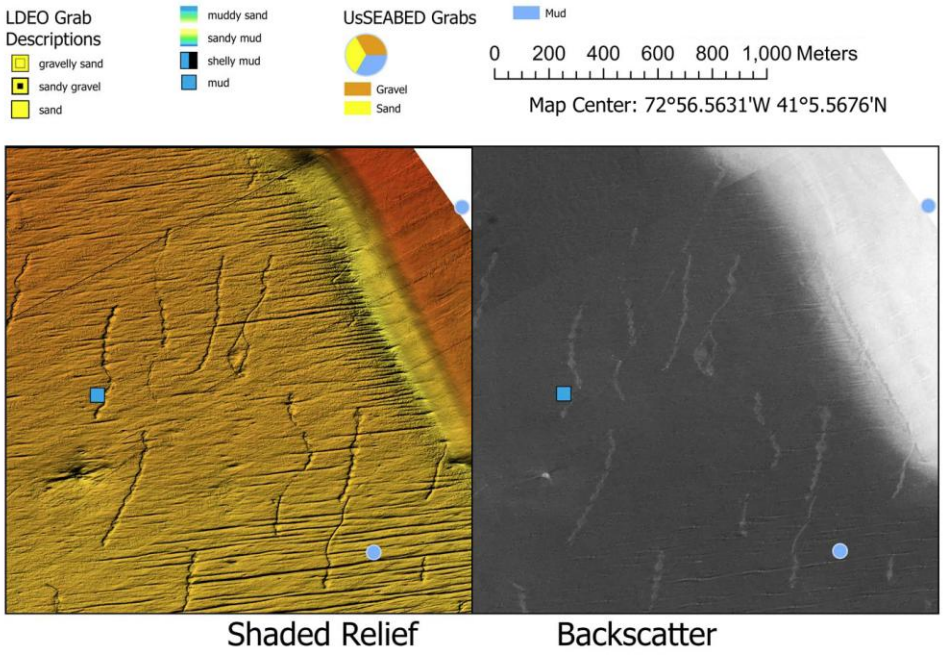

Figure 26. Furrowed seabed morphology at 28 m depth near rise with a water depth of 26 m and a depression with a water depth of 30 m. The depression and furrows at the base of the scarp appear to form in response to a stratified flow accelerating down the scarp. Also present here are north-south trending troughs with depths of about 0.2 to 0.5 m that may have formed as the thick, fine-grained post-glacial sediments that exist here compact. Left: shaded relief image showing scarp, depression, furrows and troughs. Right: multibeam backscatter mosaic showing high backscatter on rise, low backscatter in furrowed area, and higher backscatter in the trough floors.

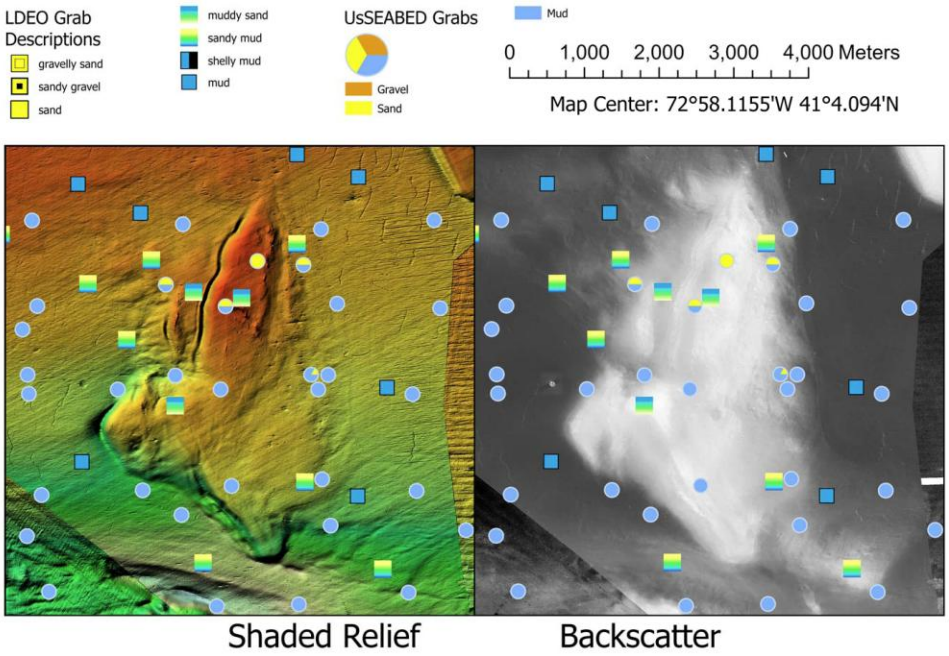

Figure 27. Detail of "Bunny Rise" in the southern portion of the Phase IV study area. The top of the higher backscatter (coarser sediment) rise sits from about 3 to 8 m above the surrounding lower backscatter (finer sediment) seafloor, which may make this an important benthic habitat. The rounded depression / rounded ridge feature at the northwest corner of the rise may have been formed by stratified flow over an abrupt topographic change.

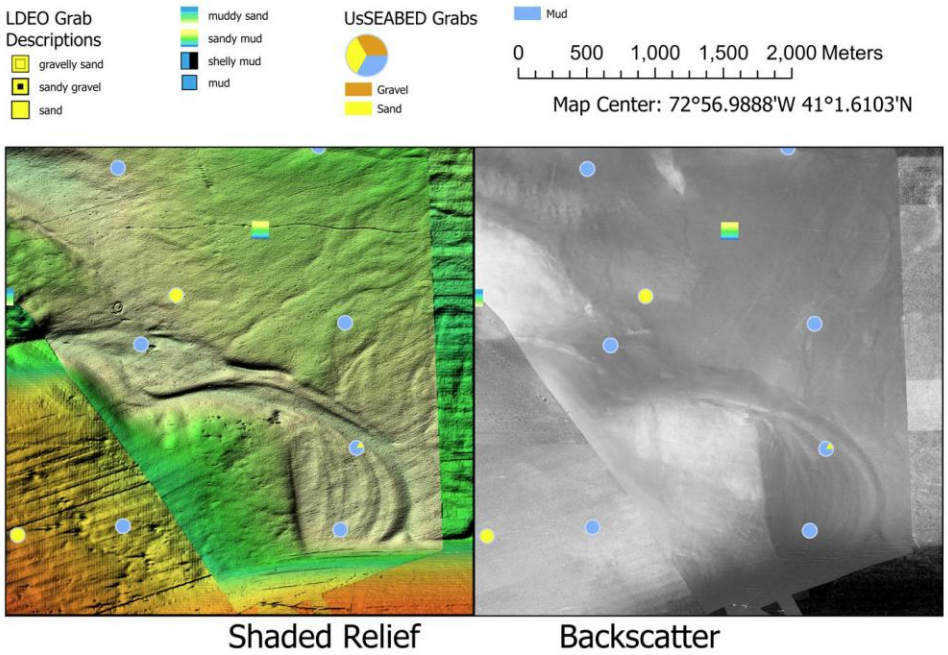

Figure 28. Detail of meandering river channel preserved at a depth of 41 m in the Phase IV study area. Left: shaded relief image near the relict channel showing the characteristic features of river beds such as meanders and meander scrolls. The channel is being buried by a modern deposit migrating to the north. One linear feature in the upper part of the area is probably an anchor drag mark and the other linear feature is a communication cable. Right: multibeam backscatter mosaic near the relict channel.

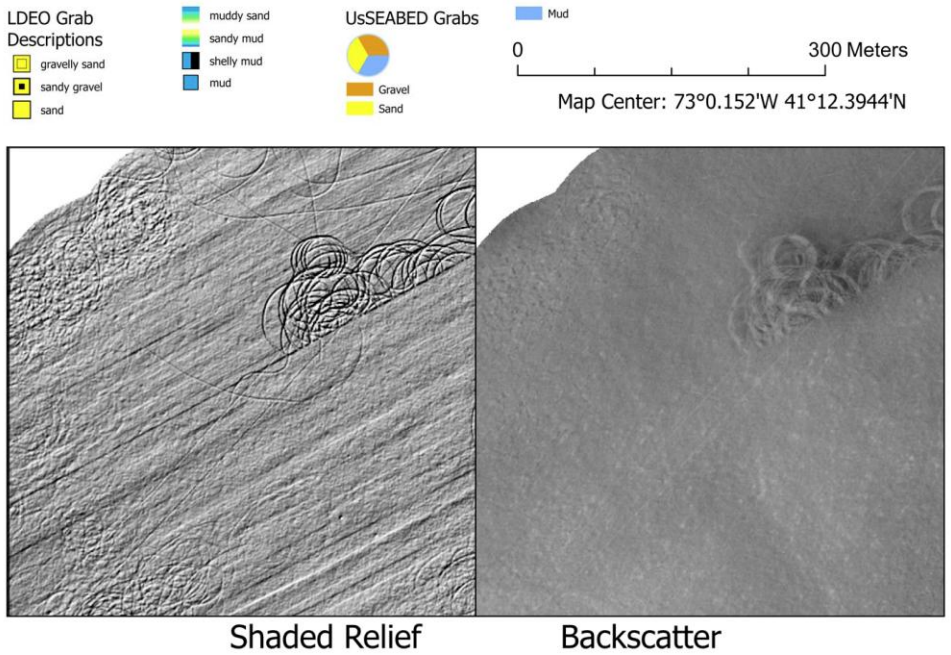

Figure 29. Recent and older shellfish dredge marks in 9 m of water near Milford. Left: shaded relief image showing recent shellfish dredge tracks which formed during the 3.5 day period after the last track that doesn't show a dredge track was surveyed. Degraded shellfish dredge tracks, probably smoothed and filled by recent sedimentation, are shown in other parts of the. Right: multibeam backscatter mosaic showing variable backscatter near recent dredge tracks and a mottled background pattern where there are degraded dredge tracks.

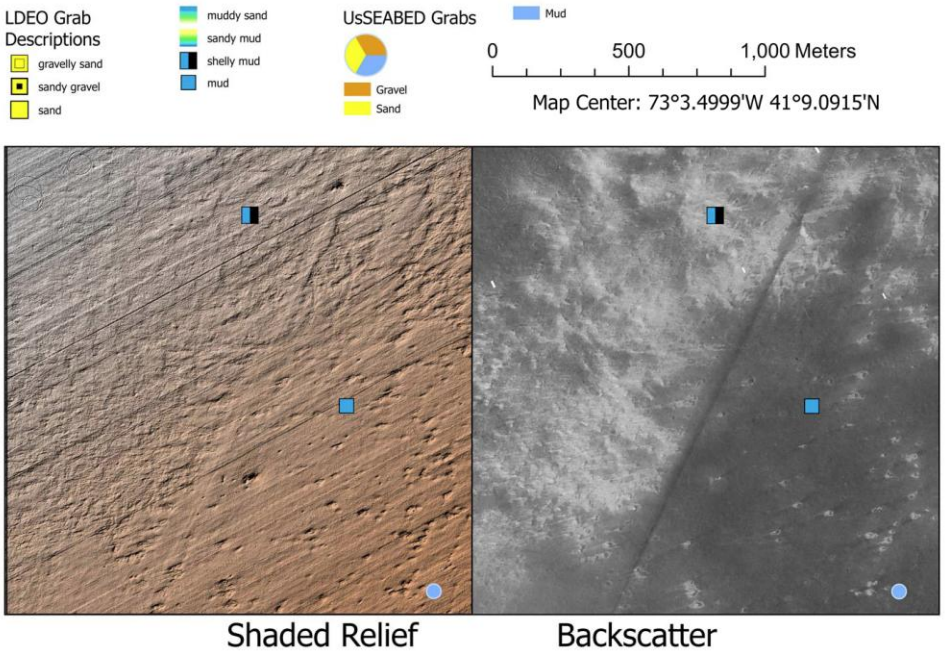

Figure 30. Degraded seafloor near the Iroquois gas pipeline. Left: shaded relief image showing an irregular seabed with some arcuate tracks and also small pits developed next to the linear pathway of the gas pipeline. Right: multibeam backscatter mosaic showing high backscatter in the degraded area which may result from erosion of the seafloor.

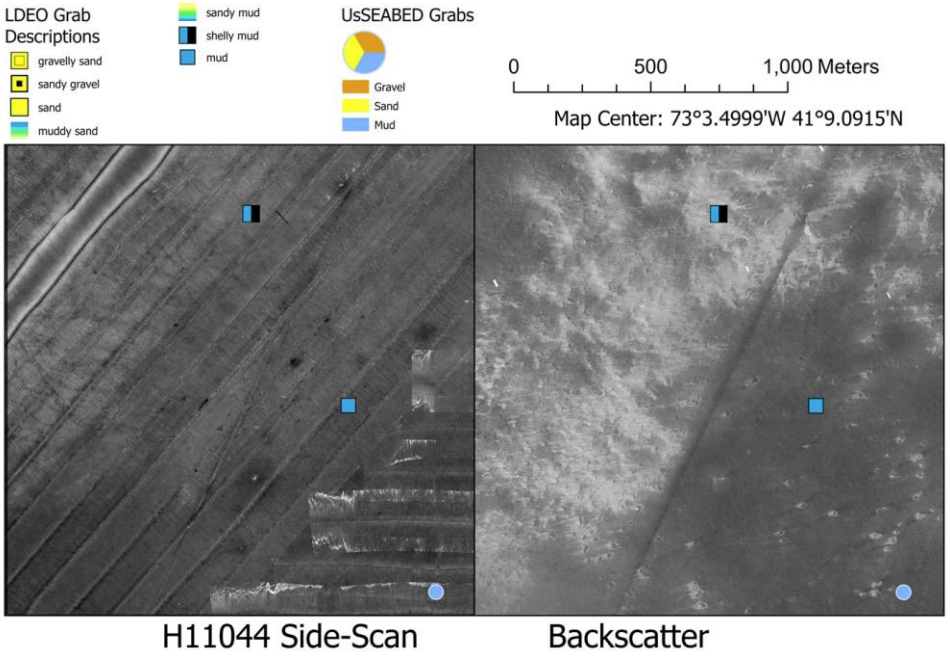

Figure 31. Left: side-scan sonar mosaic collected during NOAA hydrographic survey H11044 done in 2001 McMullen et al. (2005) showing a much different seafloor pattern, which Poppe et al. (2008) describe as dendritic channels. Cores in this general area show shelly sand layers (Poppe et al., 2008), and the erosional event that apparently occurred between 2001 and 2022 may have eroded the find-grained material so that the coarser materials are now at the surface.

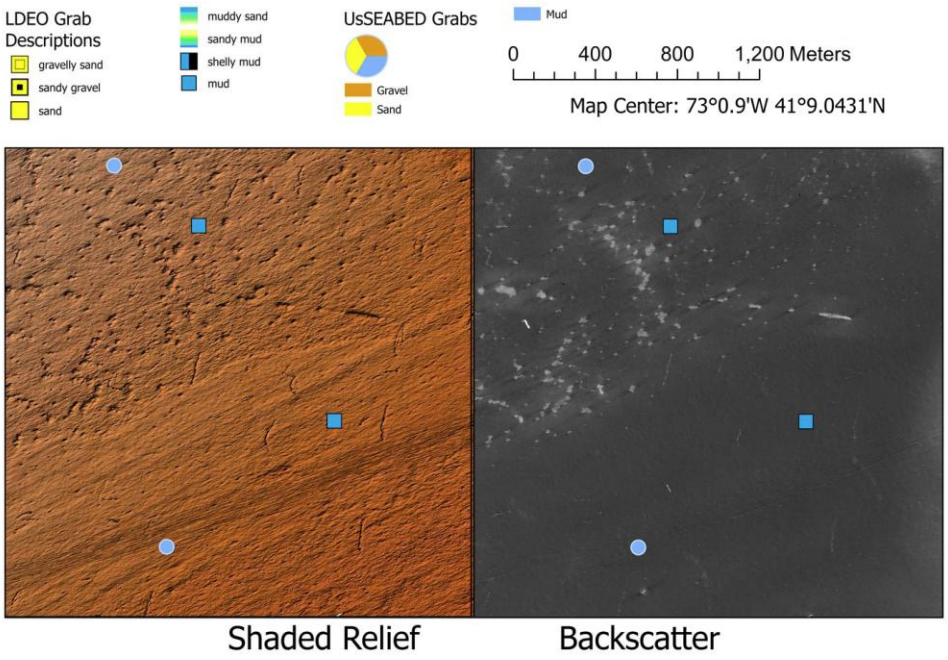

Figure 32. Variable seabed morphology in 16 m water depth suggesting local variability in sedimentation patterns. Left: shaded relief image showing a pitted seabed in the north and a slightly elevated zone of smoothed sediment in the central part of the image suggestive of more recent sediment deposition. Right: multibeam backscatter mosaic showing the characteristic elevated backscatter in the pits in the northern area but only low backscatter areas in the central area, which is consistent with more recent deposition.

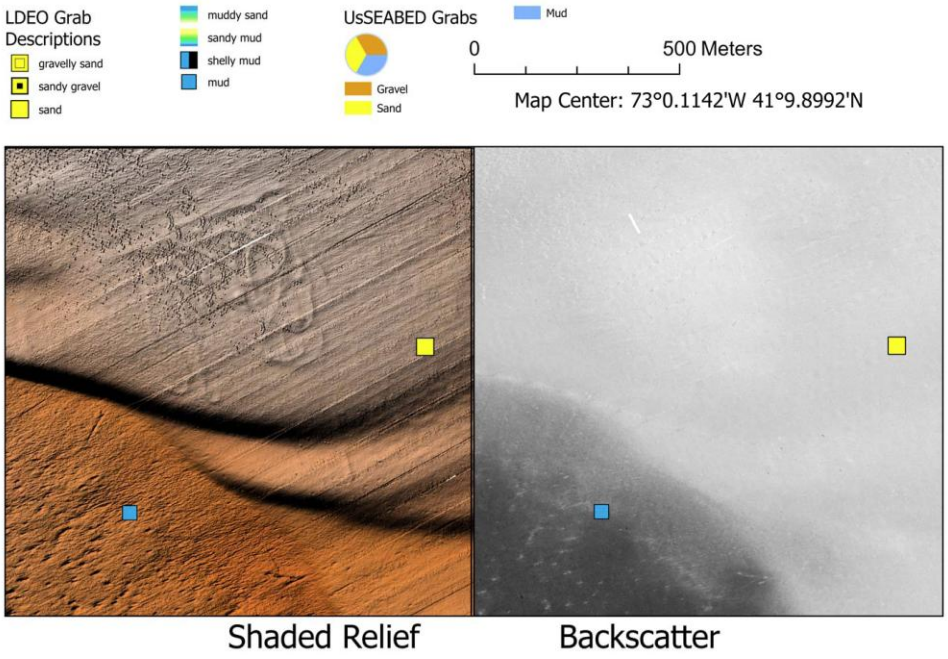

Figure 33. The multibeam mapping revealed some peculiar features on the seafloor such as the ropey deposit imaged here. Left: shaded relief image showing a feature at a water depth of 12 m that appears to be formed by materials being dropped from a ship following a rectangular course. The deposit is less than 0.2 m high. Right: multibeam backscatter mosaic showing high backscatter on the rise and low backscatter off the rise. There is apparently no backscatter signal associated with the ropey deposit suggesting that it is covered by more recent sedimentation.

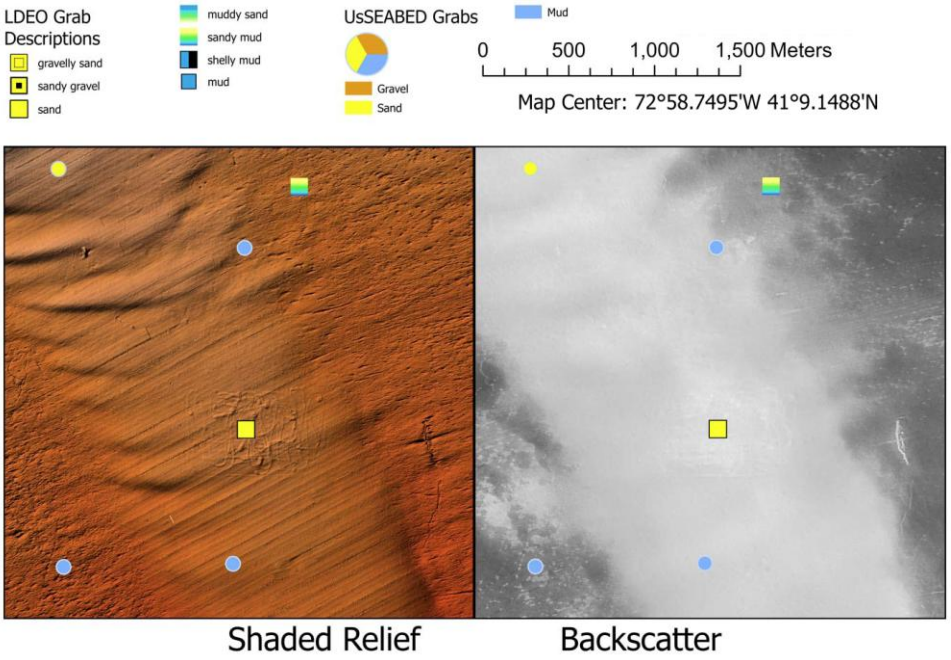

Figure 34. Another ropey deposit, here at a water depth of 16 m. Left: shaded relief image of the ropey deposit where the height is less than 0.05 m to 0.2 m. Right: multibeam backscatter mosaic showing that the deposit here shows a somewhat higher backscatter suggesting that this deposit wasn't completely buried.

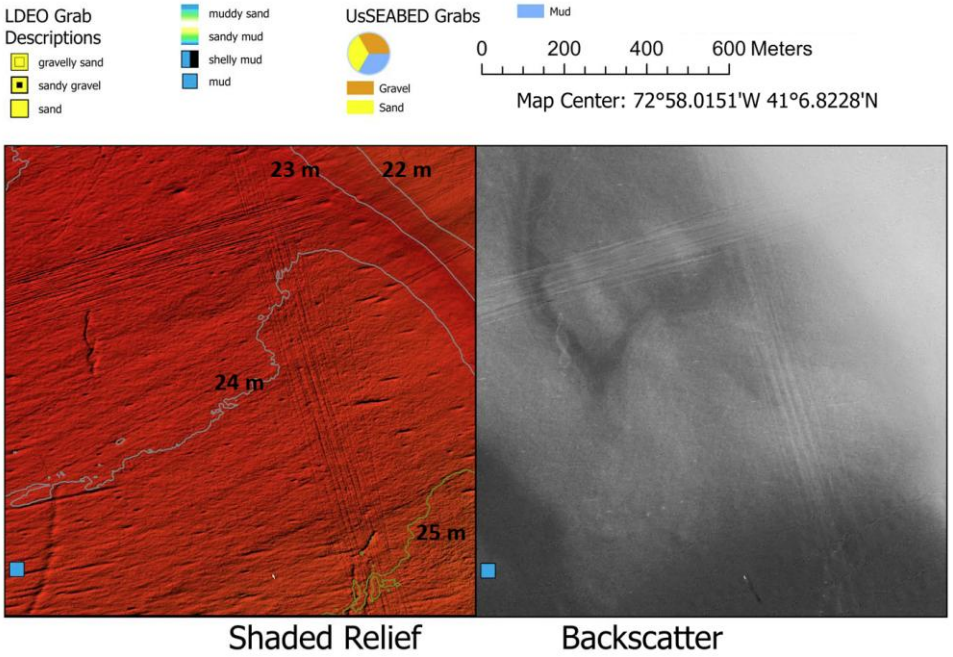

Figure 35. Another unexpected feature in the Phase IV study area are long, linear bands of drag marks. Left: shaded relief image showing two intersecting bands of linear drag marks in water depth of 24 m. It is possible that the bands are formed by barges dragging wire ropes as they travel between ports along the Connecticut shoreline. Right: multibeam backscatter mosaic showing that the drag marks have some effect on seafloor backscatter, perhaps due to roughening the seabed.

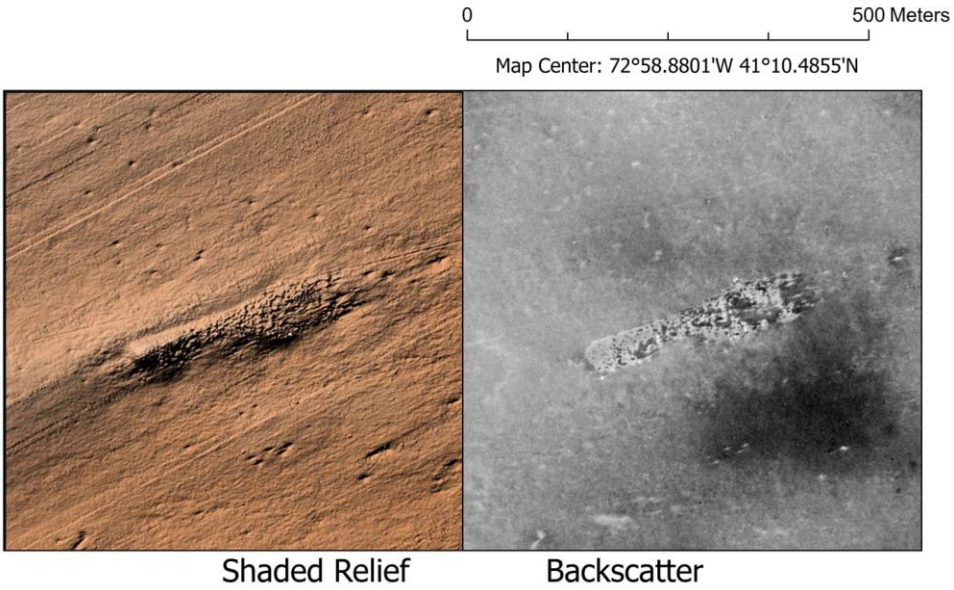

Figure 36. A striking feature imaged during the Phase IV study was a large, possibly cylindrical feature at a water depth of 14 m. The feature is labeled as a rock on the NOAA chart, but the form doesn't look like a typical rocky deposit or rock outcrop. Left: shaded relief image showing a 350 m long, 30 to 60 m wide feature that has a height of 0.25 to 0.5 m with many blocks on the eastern end of the deposit having heights of 1.0 m to 1.5 m. Right: multibeam backscatter mosaic showing an irregular backscatter pattern on the east end of the deposit, which may be due to the existence of large blocks on the deposit.

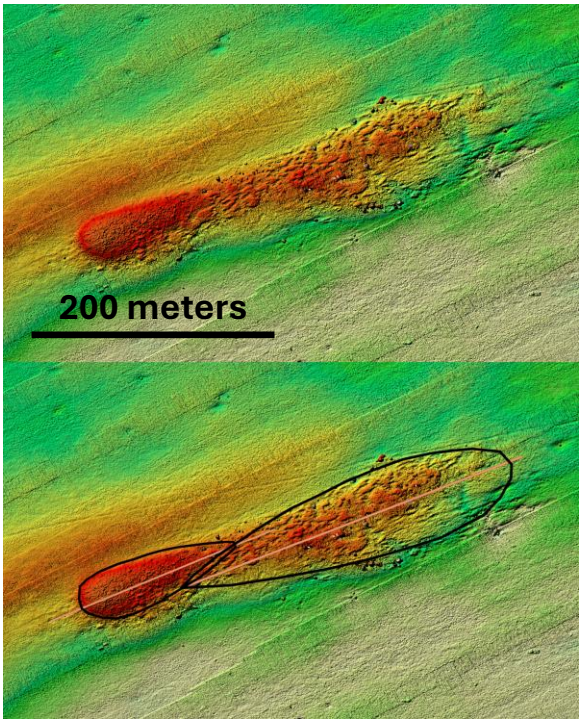

Figure 37. Hypothetical origin of this atypical seabed deposit. Upper: shaded relief image of the deposit based on depths gridded at 0.25 m. The western end of the deposit has a smoothed character while the east end of the deposit has a much lumpier texture. Lower: hypothetical origin of this feature is the result of two ship deposits; the first deposit at the west end and the second deposit, made of coarser material, on the east end.

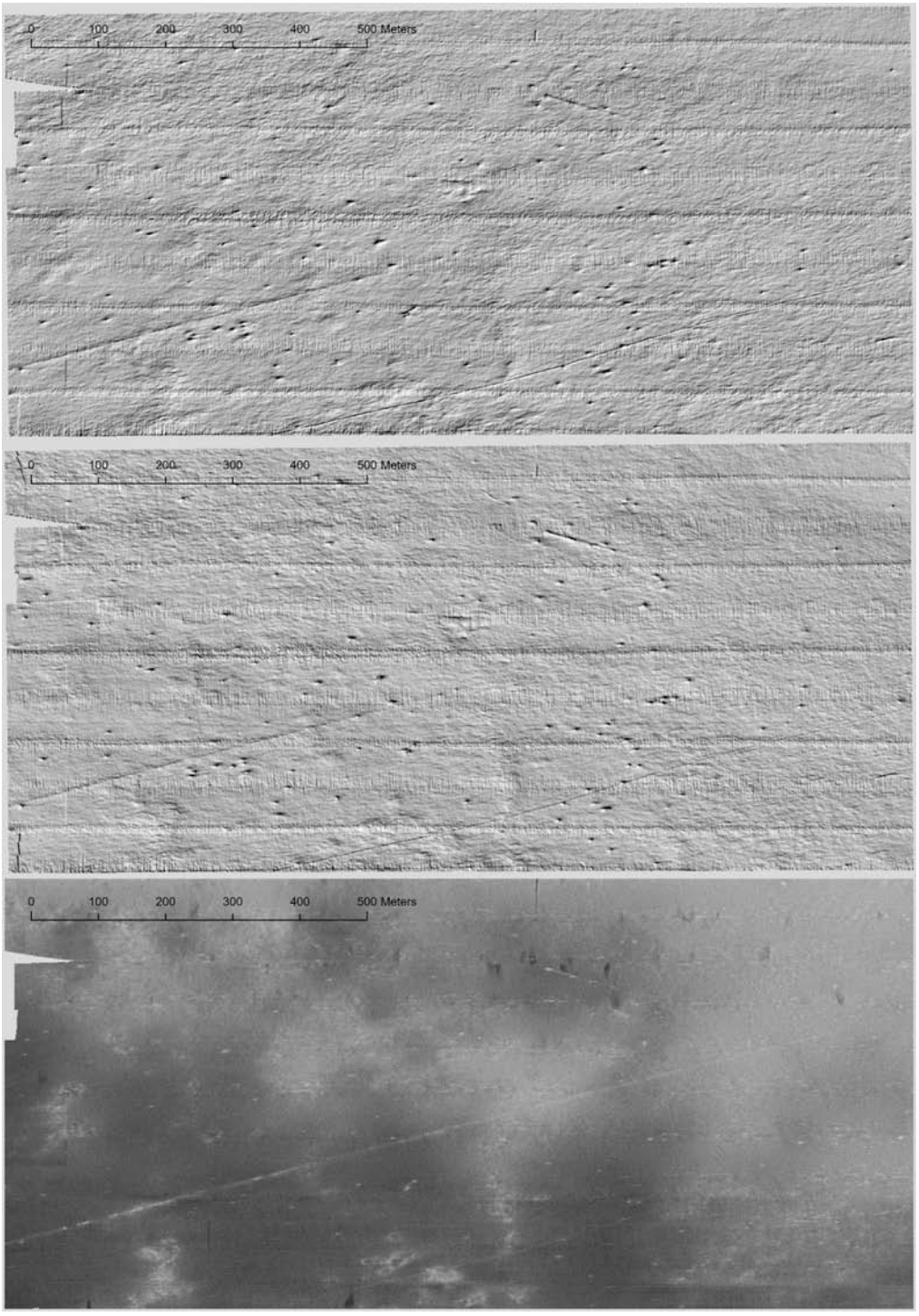

Figure A1. Multbeam survey data collected in the Reference Area in August, 2022. Upper: hillshade image of bathymetry data illuminated from the northwest. Middle: hillshade image of bathymetry data illuminated from the northeast. Lower: backscatter mosaic.

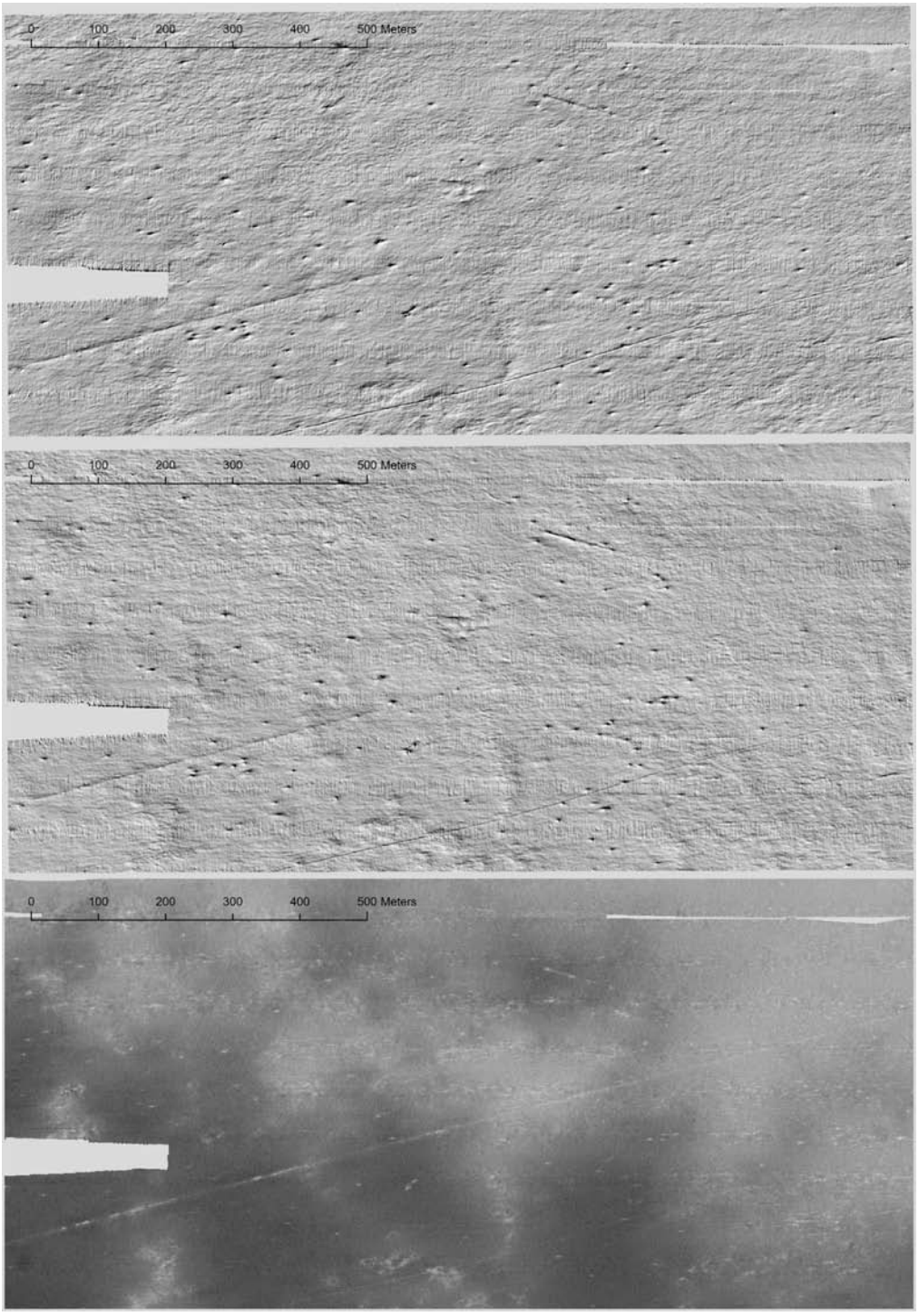

Figure A2. Multbeam survey data collected in the Reference Area in September, 2022. Upper: hillshade image of bathymetry data illuminated from the northwest. Middle: hillshade image of bathymetry data illuminated from the northeast. Lower: backscatter mosaic.

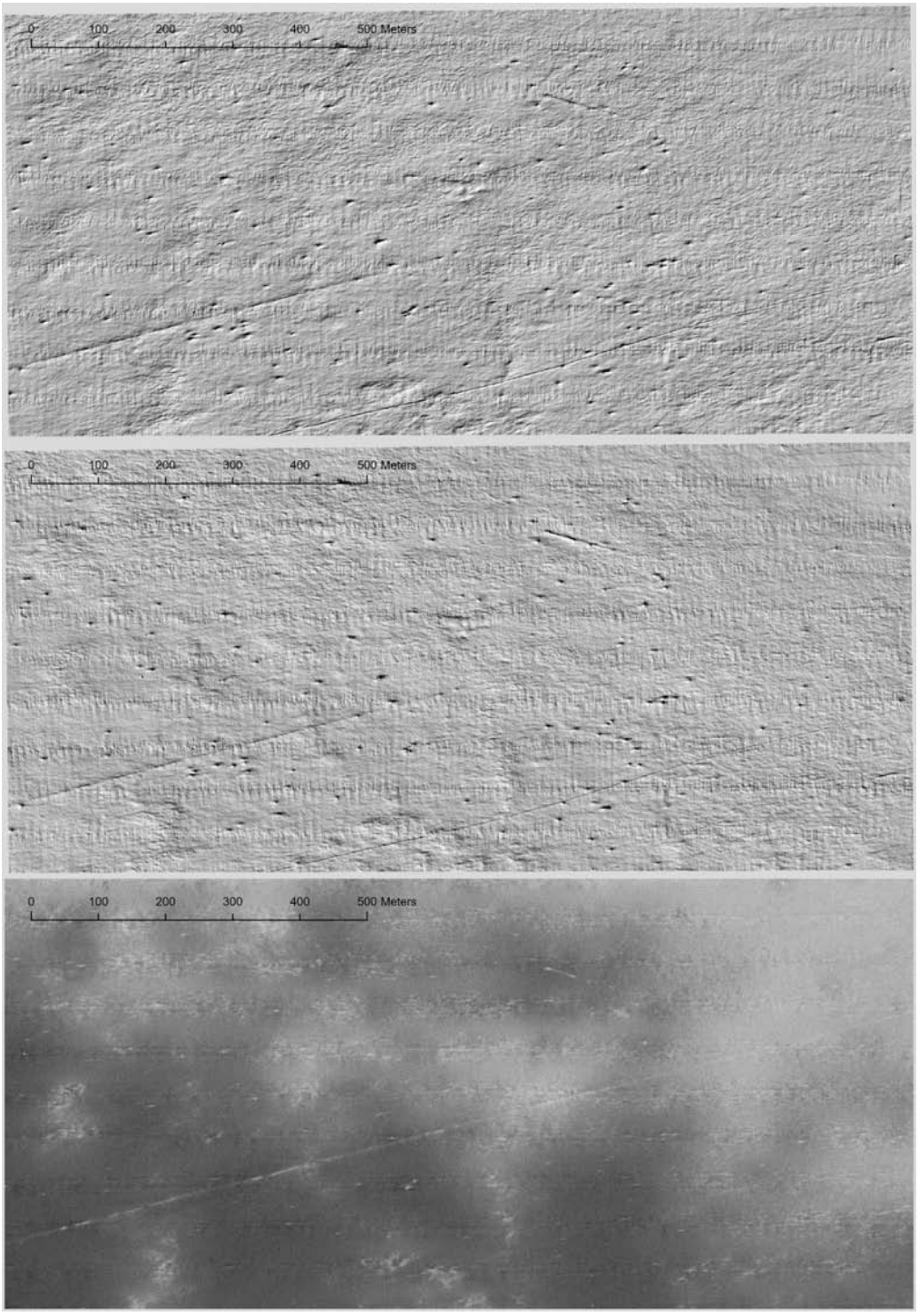

Figure A3. Multbeam survey data collected in the Reference Area in November-December, 2022. Upper: hillshade image of bathymetry data illuminated from the northwest. Middle: hillshade image of bathymetry data illuminated from the northeast. Lower: backscatter mosaic.

Figure A4. Multbeam survey data collected in the Repeat Area in August, 2022 mainline survey. Upper: hillshade image of bathymetry data illuminated from the northwest. Middle: hillshade image of bathymetry data illuminated from the northeast. Lower: backscatter mosaic.

Figure A5. Multbeam survey data collected in the Repeat Area in August, 2022 repeat survey. Upper: hillshade image of bathymetry data illuminated from the northwest. Middle: hillshade image of bathymetry data illuminated from the northeast. Lower: backscatter mosaic.